ERLER ZIMMER

3D PRINTED ANATOMY SERIES

1.0 Anatomy

Didactically colored - healthy

THE GROUND-BREAKING

Monash Anatomy Series represents an unique and unrivalled collection of colour-augmented human anatomy body replicas designed specifically for enhanced teaching and learning. This premium collection of highly accurate normal human anatomy has been generated directly from either radiographic data or actual cadaveric specimens using advanced imaging techniques. The Monash 3D Human Anatomy Series provides a cost effective means to meet your specific educational and demonstration needs in a range of curricula from medicine, allied health sciences and biological sciences. A detailed description of the anatomy displayed in each 3Dprinted body replica is provided.

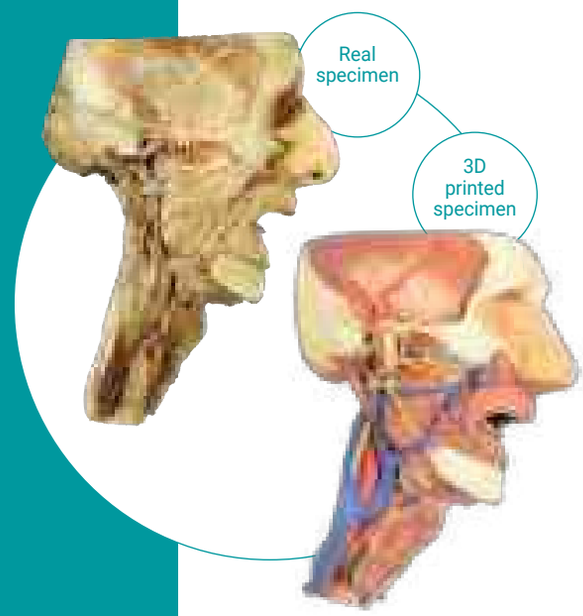

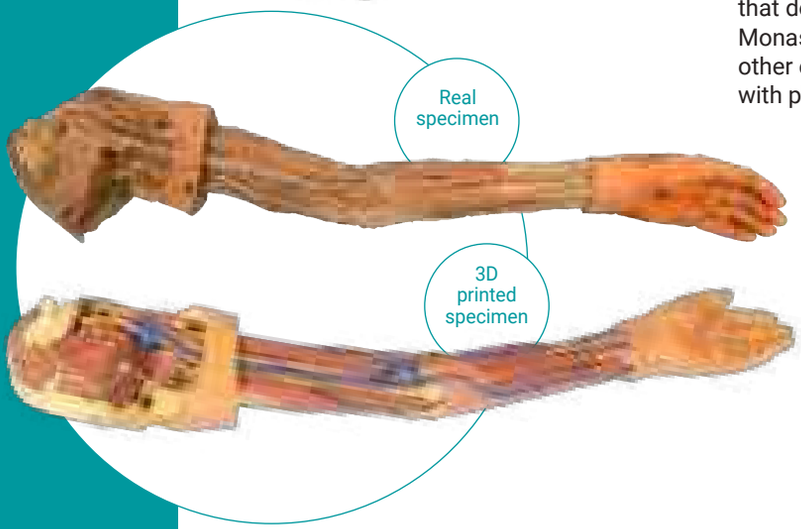

What advantages does The Monash 3D Anatomy Series offer over either plastic models or plastinated human specimens?

- ✓ Each body replica has been carefully created from selected radiographic patient data or high quality real human prosected cadaver specimens selected by a highly qualified team of anatomists at the Centre for Human Anatomy Education; Monash University to illustrate a range of clinically important areas of anatomy with a quality and fidelity that is not possible in conventional models – this is real anatomy and not stylised.
- ✓ Each body replica has been rigorously checked by a team of highly qualified anatomists at The Centre for Human Anatomy Education, Monash University, to ensure the anatomical accuracy of the final product.
- ✓ The body replicas are not real human tissue and therefore not subject to any barriers of transportation, importation or use in educational facilities that do not possess an anatomy license. The Monash 3D Anatomy Series avoids these and other ethical issues that are raised when dealing with plastinated human remains.

Head, Neck and Shoulder with angiosomes

BEST SELLER

This large 3D printed specimen displays a great deal of anatomy spanning the head, neck, thorax, axillae and upper limbs.

Item no. MP1250

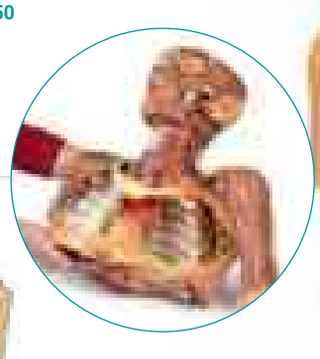

Posterior Abdominal wall

This large 3D-printed specimen displays the entire male posterior abdominal wall from the diaphragm to the pelvic brim, as well as pelvic anatomy and to the proximal thigh. This same individual specimen is also available as a pelvic and proximal thigh specimen (MP1770).

Item no. MP1300

Nervous System Dissection (posterior view)

BEST SELLER

This 3D printed specimen presents a unique view of axial anatomy, presenting a dorsal deep dissection of the head, neck, axillae, thorax, abdomen, and gluteal regions. The removal of the posterior portions of the cranium and laminectomy from the cervical region to the opening of the sacral canal affords a continuous view of the central nervous system structures and origin of the segmental nerves relative to other axillary and appendicular structures.

Item no. MP1400

Posterior Body Wall / Ventral Deep Dissection

This 3D printed specimen complements our dorsal dissection specimen (MP1400) by presenting a ventral deep dissection of axial anatomy from the head, neck, axillae, thorax, and abdomen to the proximal portion of the thighs. The removal of the anterior portions of the cranium and vertebral bodies from the cervical region to the 5th lumbar provides a continuous view of the central nervous system structures and origin of the segmental nerves relative to other axillary and appendicular structures.

Item no. MP1410

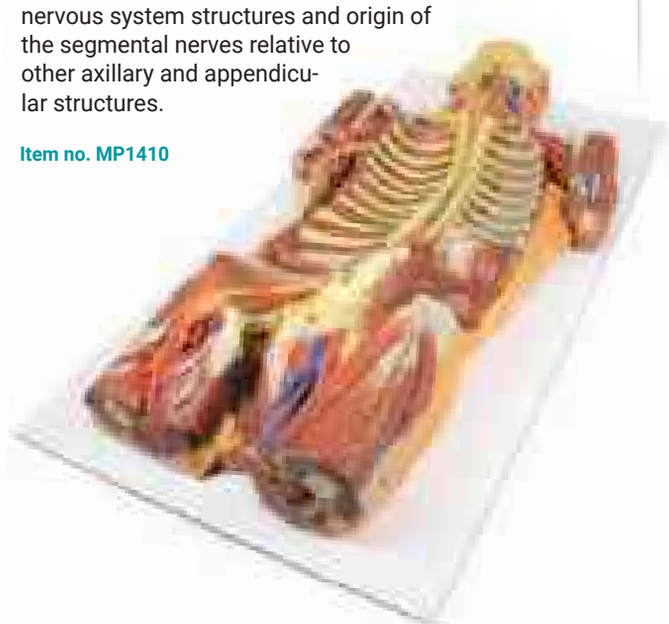

Hand

BEST SELLER

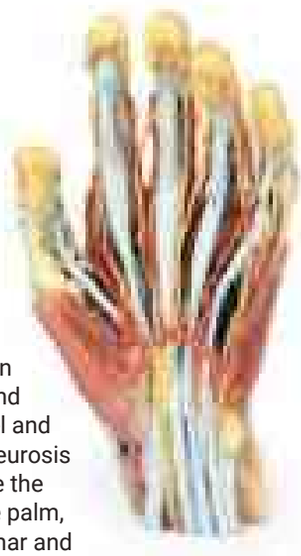

This 3D printed specimen demonstrates a superficial dissection of a left hand and wrist. Anteriorly, the transverse carpal and palmar carpal ligaments have been removed to expose the tendons and nerves traversing the carpal tunnel and Canal of Guyon. The palmar aponeurosis has been removed to demonstrate the course of the tendons through the palm, the superficial muscles of the thenar and hypothenar eminences (abductors and flexors), and the lumbrical muscles arising from the flexor digitorum tendon.

Item no. MP1530

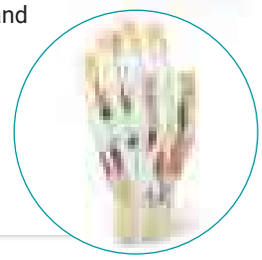

Forearm and hand

– superficial and deep dissection.

This 3D printed specimen preserves a mixed superficial and deep dissection of the anterior aspect of a right distal arm, forearm and hand.

Item no. MP1512

Forearm and hand

– deep dissection. This 3D printed specimen of a left upper limb preserves a deep dissection from the distal humerus to the palmar surface of hand.

Item no. MP1514

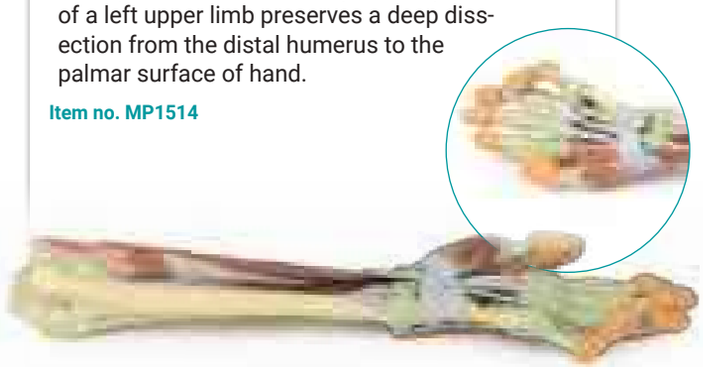

Upper Limb

This 3D-printed specimen demonstrates the superficial anatomy of a left upper limb from the blade of the scapula to the hand. The skin and superficial and deep fascia has been removed from most of the limb except over the dorsum of the scapula, proximal arm, and over the hand. The superficial veins, including the median cubital vein, have been maintained; with the cephalic and basilica preserved from the wrist to the deltopectoral groove and termination in the brachial vein, respectively.

Item no. MP1500

Upper limb and hand

– deep dissection.

This 3D print of a superficially dissected right upper limb specimen displays a mixture of the vascular, nervous and muscular anatomy of the distal arm, forearm and hand.

Item no. MP1513

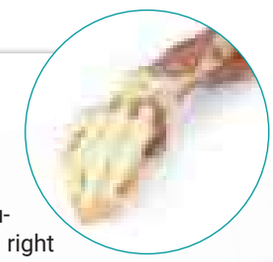

Upper Limb – elbow, forearm and hand

This 3D-printed specimen displays a great deal of upper limb anatomy. In the distal arm and elbow/cubital fossa region it shows the arrangement of the biceps tendon, brachial artery and median nerve arranged from lateral to medial. The bicipital aponeurosis has been divided to reveal the structures deep to it.

Item no. MP1510

Upper Limb Ligaments

This 3D printed specimen presents the entire upper limb skeleton and ligaments from the pectoral girdle to the hand. Detailed anatomical description on request.

Item no. MP1520

Upper Limb – biceps, bones and ligaments

This 3D-printed specimen shows the origin and insertion of biceps (most other arm and shoulder muscle bellies have been removed). The long head of biceps arises from the supraglenoid tubercle (hidden from view) and travels inferiorly in the bicipital groove, whereas the short head of biceps arises from the coracoid process. The bifid insertion of the muscle as the bicipital aponeurosis and the rounded tendon which can be seen winding around the radius to insert into the radial tuberosity are clearly discernable.

Item no. MP1515

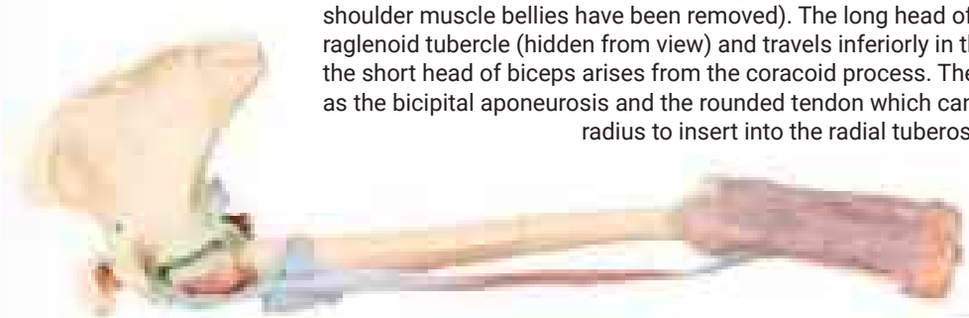

Cubital Fossa

This 3D printed cubital fossa displays a superficial dissection of the right distal arm and proximal forearm. The skin and superficial fascia has been removed anteriorly, medially and laterally to expose the superficial veins (basilic, cephalic, and median cubital) and cutaneous (medial, lateral and posterior antebrachial) nerves.

Item no. MP1750

Cubital fossa – muscles, large nerves and the brachial artery

This 3D printed specimen presents a left distal arm and proximal forearm with all skin, subcutaneous fat and superficial cutaneous nerves and veins removed. The elbow region partially flexed to display the arrangement of muscles and neurovascular structures of the cubital fossa.

Item no. MP1755

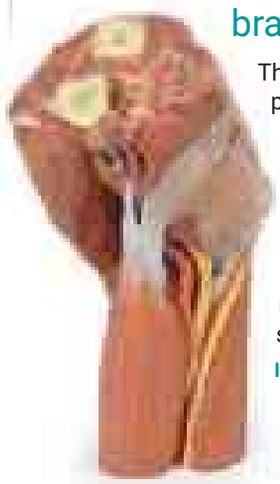

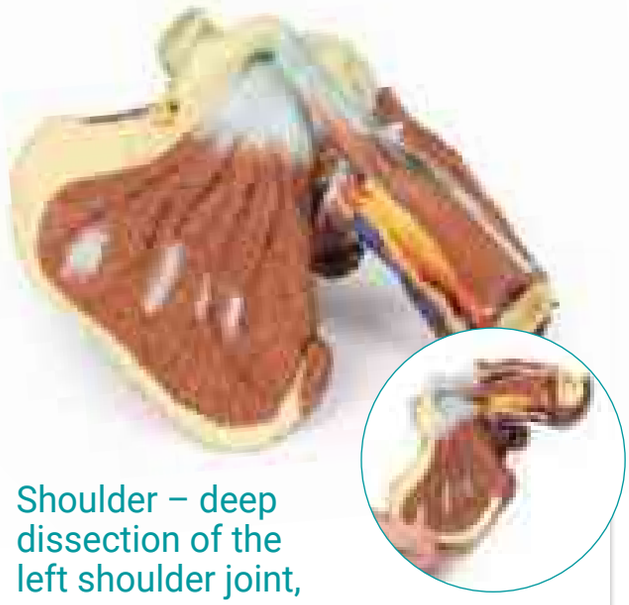

Shoulder – deep dissection of the left shoulder joint,

musculature, and associated nerves and vessels.
This 3D printed specimen presents a deep dissection of the left shoulder joint, musculature, and associated nerves and vessels of the scapula and proximal humerus (to near midshaft). Anteriorly, the deltoid muscle has been detached from its origin to expose the underlying deeper structures of the shoulder joint and rotator cuff musculature.

Item no. MP1525

Shoulder – deep dissection of a right shoulder girdle,

preserving a complete scapula, lateral clavicle, and proximal humerus. This 3D printed specimen preserves a deep dissection of a right shoulder girdle, consisting of a complete scapula, lateral clavicle, and proximal humerus. In the anterior view, the subscapularis muscle is present but sectioned to highlight the cross-sectional thickness of the belly within the subscapular fossa.

Item no. MP1527

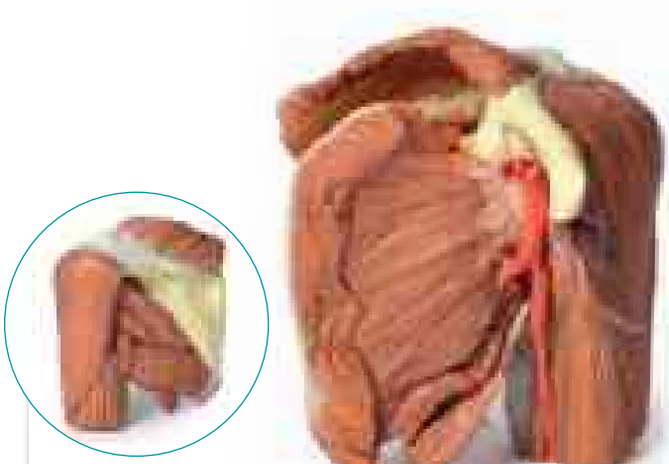

Shoulder left – Superficial muscles and axillary/brachial artery

This printed 3D left shoulder specimen consists of the scapula, humerus (sectioned near midshaft) and clavicle (sectioned at midshaft) with the superficial muscles around the shoulder joint, the rotator cuff muscles and the axillary artery as it progresses distally to become the brachial artery. The muscles attached to the clavicle have been preserved including the subclavius muscle attachment to the inferior border of the clavicle and the deltoid covering the lateral aspect of the proximal upper limb (overlying the origins of the long head of biceps brachii and the lateral head of triceps brachii).

Item no. MP1523

Right thoracic wall – axilla, and the root of the neck

This 3D printed specimen preserves a dissection of the right thoracic wall, axilla, and the root of the neck. Structures within the right chest wall are visible deep to the parietal pleura, including the ribs, muscles of the intercostal spaces and the origins of the neurovascular bundle in each intercostal space. The pectoralis major has been reflected medially towards the sectioned edge of the specimen to expose pectoralis minor which acts as a useful landmark as it divides the axillary artery into its three parts. The clavicle has had its middle 1/3 removed, but the subclavius muscle has been retained. The brachial plexus and many of its branches are seen almost in its entirety from the roots of C5-T1 to its termination.

Item no. MP1521

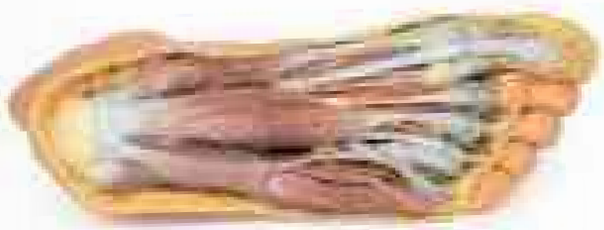

Foot – Plantar surface

and superficial dissection on the dorsum.
This 3D printed specimen is a left foot with superficial structures exposed on the dorsum, and the superficial layer of muscles and nerves on the plantar surface. The anterior portion of the plantar aponeurosis has largely been removed to expose the first layer of muscles.

Item no. MP1910

Foot – Deep plantar structures

This 3D printed specimen provides a view of deep plantar structures of a right foot. Medially, the cut edge of the great saphenous vein is visible within the superficial fascia, just anterior to the cut edges of the medial and lateral plantar arteries and nerves overlying the insertion of the tibialis posterior muscle. The superficial fascias, the plantar aponeurosis, and superficial musculature have been removed to expose the deep (third layer) of musculature.

Item no. MP1940

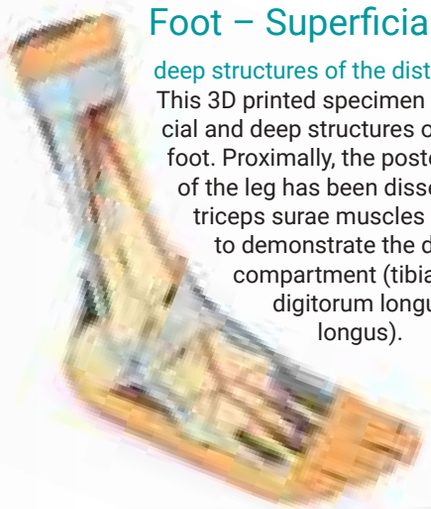

Foot – Superficial and

deep structures of the distal leg and foot.
This 3D printed specimen presents both superficial and deep structures of a right distal leg and foot. Proximally, the posterior compartment of the leg has been dissected to remove the triceps surae muscles and tendocalcaneous to demonstrate the deep muscles of the compartment (tibialis posterior, flexor digitorum longus, flexor hallucis longus).

Item no. MP1930

Foot – Superficial and

deep dissection of distal leg and foot.
This 3D printed specimens preserves a mixed superficial and deep dissection of a left distal leg and foot. Posteriorly, the compartment muscles and neurovascular structures have been removed to isolate the tendocalcaneous and expose the body of the calcaneus.

Item no. MP1920

Foot – Structures of the plantar surface

This 3D print records the anatomy of a right distal leg and the deep structures of the plantar surface of the foot. Proximally, the tibia, fibula, interosseous membrane, and leg muscles are discernable in cross-section. Medially, at the level of the ankle joint, the long tendons of the dorsi- and plantar-flexors are visible superficial to the capsular and extra capsular ligaments.

Item no. MP1900

Foot – Parasagittal cross-section

This 3D printed specimen provides a parasagittal cross-section through the medial aspect of the right distal tibia and foot, displaying the skeletal structures of the medial longitudinal arch of the foot and surrounding soft-tissue structures.

Item no. MP1850

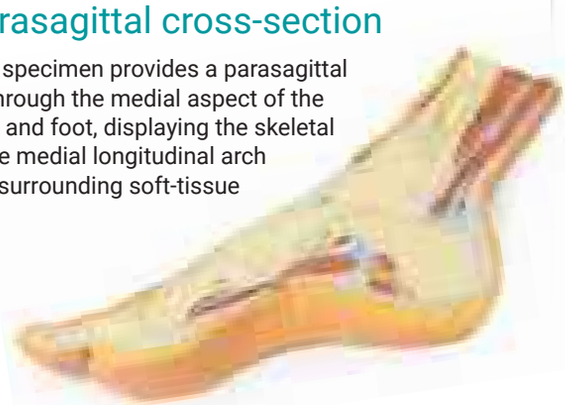

Lower Limb – deep dissection

This 3D printed specimen consists of a right partial lower limb sectioned just proximal to the knee joint and complete through a partially dissected foot exposing the structures on the dorsum.

Item no. MP1809

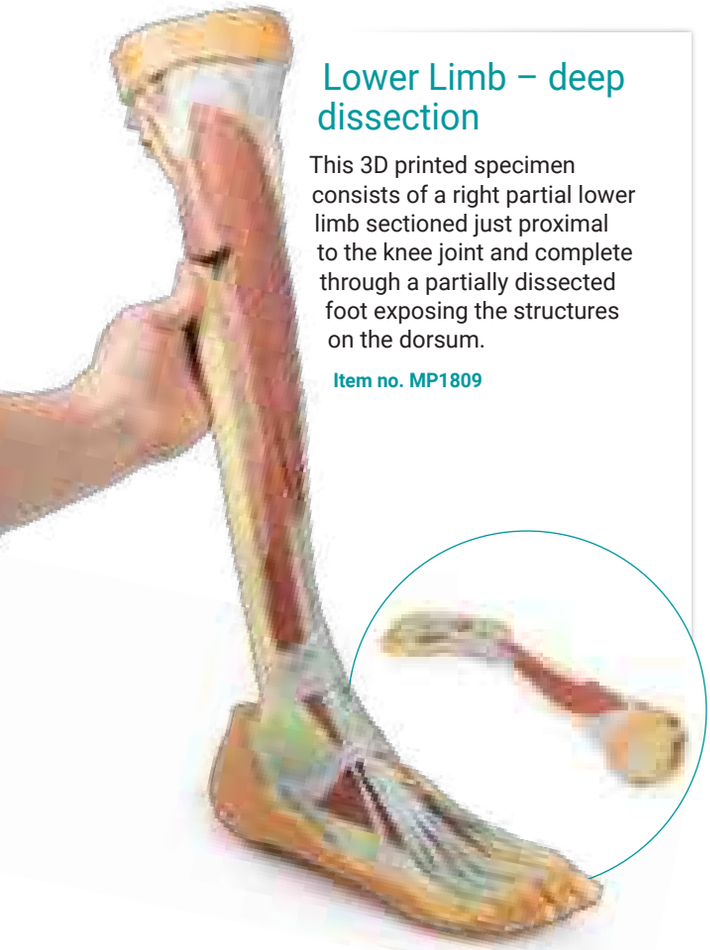

Lower Limb superficial veins

This 3D printed specimen presents a superficial dissection of a left lower limb, from just proximal to the knee joint to a complete foot. The skin and superficial fascia have been removed to display the superficial venous structures of the leg including the dorsal venous plexus, great saphenous vein (including numerous tributaries), and the small saphenous vein (including numerous tributaries) on the crural fascia.

Item no. MP1815

Lower limb – superficial dissection

This 3D printed specimen represents the remainder of the lower limb portions of our male abdominopelvic and proximal thigh specimen (MP1765), sectioned proximally near midthigh and continuous to the partially dissected foot. The transverse section through the thigh exposes the neurovascular structures of the anterior, medial and posterior compartments.

Item no. MP1816

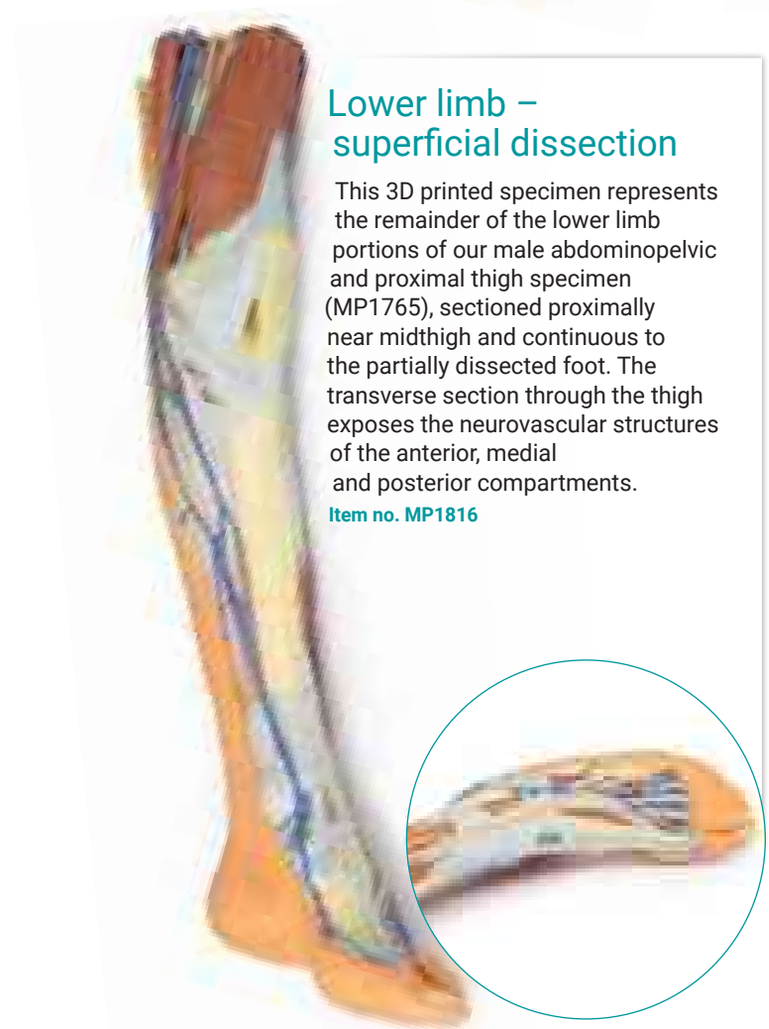

Lower Limb Musculature

This 3D printed specimen preserves a superficial dissection of the lower limb musculature from the mid-thigh to mid-leg, as well as nerves and vessels of the popliteal fossa. The insertions of the muscles of the anterior, middle and posterior compartments of the thigh are visible, including the pes anserinus medially and the iliotibial tract laterally. The capsule of the knee joint has been opened anteriorly to demonstrate the menisci and the tibial and fibular collateral ligaments. Detailed anatomical description on request.

Item no. MP1810

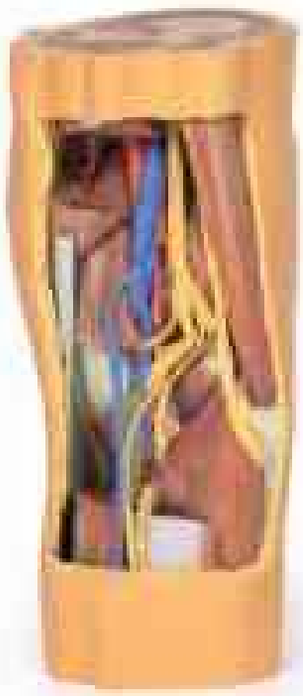

Popliteal Fossa distal thigh and

proximal leg. This 3D printed specimen preserves the distal thigh and proximal leg, dissected posteriorly to demonstrate the contents of the popliteal fossa and surrounding region.

Item no. MP1820

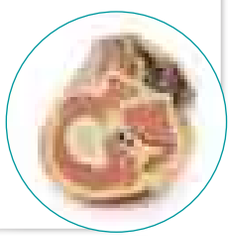

BEST SELLER

Popliteal Fossa

This 3D printed specimen preserves the distal thigh and proximal leg, dissected posteriorly to demonstrate the contents of the popliteal fossa and surrounding region. The proximal cross-section demonstrates the anterior, posterior and medial compartment muscles, with the femoral artery and vein visible within the adductor canal. The sciatic nerve and great saphenous vein are also visible.

Item no. MP1830

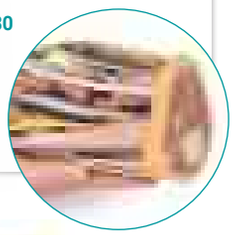

Flexed knee joint deep dissection

This 3D printed specimen displays a deep dissection of a left knee joint with the internal joint capsule structures relative to superficial tissues in a flexed position.

Item no. MP1807

Knee Joint, flexed

This 3D printed specimen demonstrates the ligaments of the knee joint with the leg in flexion. In the anterior view, with the patella and part of the patellar ligament removed, the medial and lateral menisci and anterior and posterior cruciate ligaments are visible.

Item no. MP1800

Knee Joint, extended

This 3D printed specimen demonstrates the ligaments of the knee joint with the leg in extension; it represents the same specimen as MP1800 knee joint printed in a flexed position. Both tibial and fibular collateral ligaments are intact.

Item no. MP1805

Male left pelvis and proximal thigh

This 3D printed male left pelvis and proximal thigh (sectioned through the midsagittal plane in the midline and transversely through the L3/4 intervertebral disc) shows superficial and deep structures of the true and false pelves, inguinal and femoral region. In the transverse section, the epaxial musculature, abdominal wall musculature (rectus abdominis, external and internal abdominal obliques, transversus abdominis), psoas major and quadratus lumborum are visible and separated from each other and the superficial fat by fascial layers such as the rectus sheath and the thoracolumbar fascia. The psoas major muscle lies lateral to the external iliac artery, with the left testicular artery and vein lying on its superficial surface. More laterally (and moving inferiorly), the ilioinguinal nerve, the lateral cutaneous nerve of the thigh and the femoral nerve are positioned over the superficial surface of the iliacus muscle.

Item no. MP1765

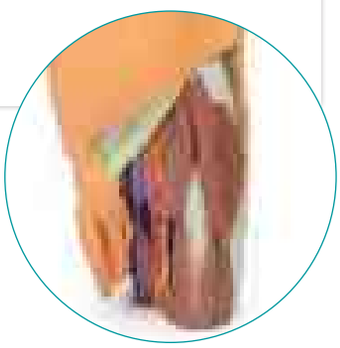

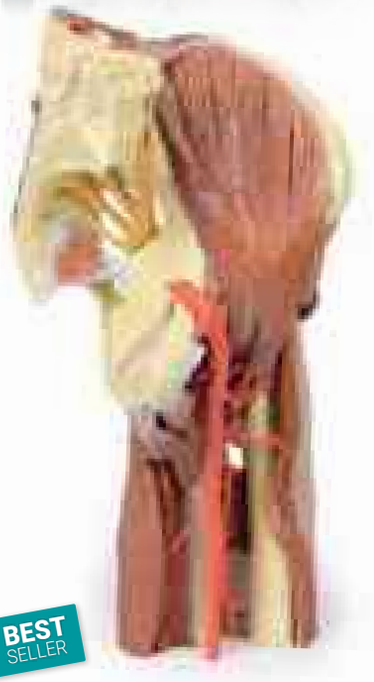

BEST SELLER

Lower Limb – deep dissection of a left pelvis and thigh

This 3D printed specimen presents a deep dissection of a left pelvis and thigh to show the course of the femoral artery and sciatic nerve from their proximal origins to the midshaft of the femur. Proximally, the pelvis has been sectioned along the mid-sagittal plane and the pelvic viscera are removed. In the pelvis the coccygeus muscle spans between the sacrum and iliac spine and the obturator artery and nerve entering the obturator canal superior to the obturator membrane.

Item no. MP1813

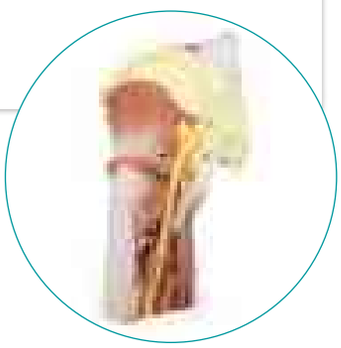

Lower limb – superficial dissection with male left pelvis

This 3D printed specimen combines the Lower limb – superficial dissection (Ref.no. MP1816) with the male left pelvis (Ref.no. MP1765).

Item no. MP1818

Female left pelvis and proximal thigh

This 3D printed female left pelvis and proximal thigh preserves both superficial and deep structures of the true and false pelves, inguinal region, femoral triangle, and gluteal region. The specimen has been sectioned transversely through the fourth lumbar vertebra, displaying the cross-section of the musculature (epaxial musculature, psoas and quadratus lumborum muscles) and cauda equina within the vertebral canal. The ventral and dorsal roots of the cauda equina are also visible exiting the intervertebral and sacral foramina in the sagittal section.

Item no. MP1780

Female right pelvis superficial and deep structures

This 3D printed female right pelvis preserves both superficial and deep structures of the true and false pelves, as well as the inguinal ligament, the obturator membrane and canal, and both the greater and lesser sciatic foramina. Somewhat unique is the removal of portions of the peritoneum (a grayish colour) to create 'windows' displaying extraperitoneal structures.

Item no. MP1783

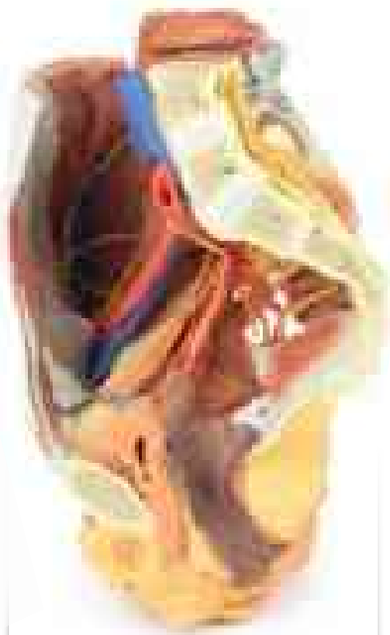

Female right pelvis

This 3D printed specimen represents a female right pelvis, sectioned along the midsagittal plane and transversely across the level of the L4 vertebrae and the proximal thigh. The specimen has been dissected to demonstrate the deep structures of the true and false pelves, the inferior anterior abdominal wall and inguinal region, femoral triangle and gluteal region.

Item no. MP1785

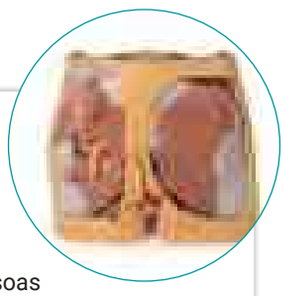

Male Pelvis

This 3D printed specimen represents the inferior posterior abdominal wall, the pelvic cavity and the proximal thigh. The common iliac veins unite to form the inferior vena cava. The iliacus and psoas muscles are easy to identify, the latter has a prominent psoas minor tendon. The nerves of the iliac fossa and their course is clearly visible, as is the genitofemoral nerves on the surface of psoas muscle. The ureters also descend on the superficial surface of the psoas and cross from its lateral to its medial border. They enter the pelvis at the bifurcation of the common iliac arteries into external and internal arteries. The external iliac arteries and veins running along the pelvic brim are clearly visible, as is the vas deferens crossing the brim from the deep inguinal ring to enter the pelvis.

Item no. MP1770

Heart

This 3D printed heart specimen preserves superficial cardiac anatomy and the bases of the great vessels. All four chambers (atria and ventricles) are preserved, with the pericardial reflections on the left atrium demarcating the position of the transverse and oblique pericardial sinuses. On the posterior aspect, the coronary sinus receives all the cardiac veins (great, middle, small) and a prominent posterior vein of the left ventricle. The aortic and pulmonary semilunar valves are visible at the bases of the ascending aorta and pulmonary trunk, respectively.

Item no. MP1700

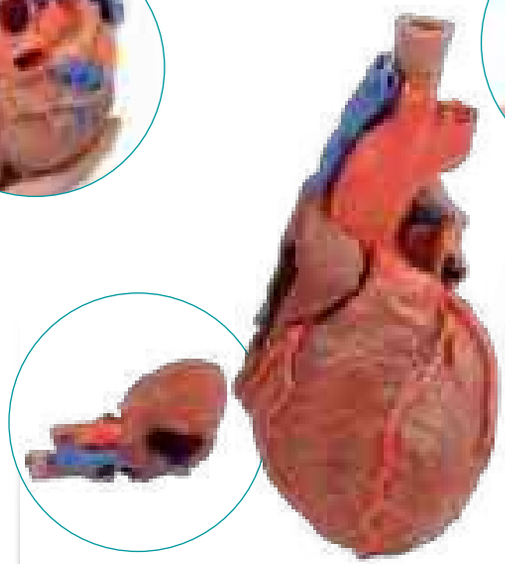

Heart and the distal trachea, carina and primary bronchi

This 3D printed specimen preserves the external anatomy of the heart and the distal trachea, carina, and primary bronchi in the posterior mediastinum relative to the great vessels and left atrium The left auricle has been sectioned to demonstrate the course of the circumflex artery in the coronary groove. The pulmonary trunk has been removed to expose the (open) pulmonary semilunar valves, while the arch of the aorta is intact to display the origins of the brachiocephalic trunk, left common carotid, and left subclavian.

Item no. MP1710

Heart internal structures

This 3D printed heart has been dissected to display the internal structures of the chambers. At the base of the heart the termination of the superior vena cava is preserved entering the right atrium. Part of the inferior vena cava is also preserved on the inferior aspect of the right atrium; however, most of the vessel lumen and much of the anterior wall has been removed to expose the pectinate muscles of the right auricle and the fossa ovalis. The anterior wall of the right ventricle has also been removed.

Item no. MP1715

BEST SELLER

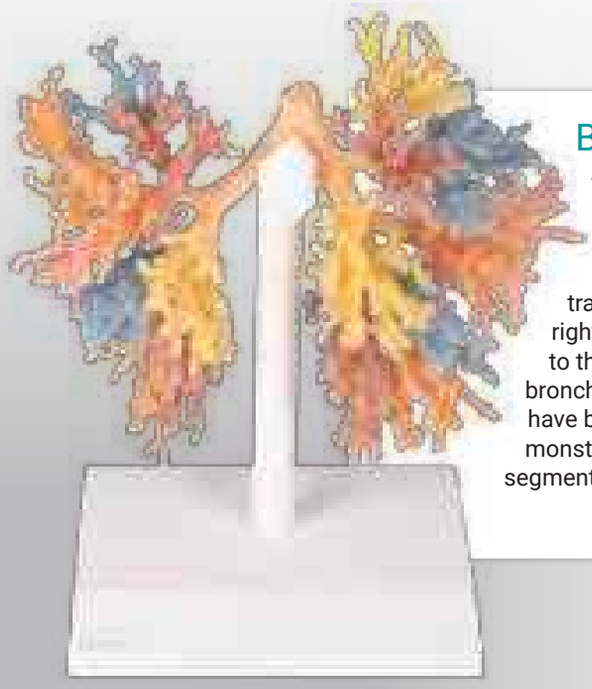

Bronchial Tree

This 3D printed specimen presents the conducting pathways of the respiratory system from the trachea, carina, and complete right and left bronchial trees to the level of the tertiary lobar bronchi. Each set of lobar bronchi have been colour-coded to demonstrate the bronchopulmonary segments of the right and left lobes.

Item no. MP1690

Bowel – Portion of Ileum

This 3D printed specimen demonstrates a small loop of ileum and mesentery. A window into the mesentery has been dissected (removing fat and visceral peritoneum) to show arterial arcades in the mesentery.

Item no. MP1725

Bowel – Portion of Jejenum

This 3D printed specimen presents a small loop of jejenum and mesentery. A window into the mesentery, fat and visceral peritoneum has been removed to illustrate the arterial arcades in the mesentery.

Item no. MP1730

Head and visceral column of the neck

This 3D print specimen preserves a series of features of the head and visceral column of the neck: The face: On the right side of the head the parotid gland has been removed to reveal the facial nerve and all its branches (temporal, zygomatic, buccal, marginal mandibular and cervical) and demonstrate the spatial relations of structures embedded in the gland from superficial to deep (facial nerve, retromandibular vein, external carotid artery). In the surrounding region the temporalis, masseter and posterior belly of digastric are exposed, as are and the facial artery, transverse facial artery and superficial temporal artery. The facial vein and transverse facial vein are clearly visible uniting to form the common facial vein which is joined by the retromandibular vein to form the external jugular vein.

Item no. MP1670

Deep face/ Infratemporal fossa

In this 3D printed specimen of a midsagittally-sectioned right face and neck, the ramus, coronoid process and head of the mandible have been removed to expose the deep part of the infratemporal fossa. The pterygoid muscles have also been removed to expose the lateral pteygoid plate and posterior surface of the maxilla. The buccinator has been retiained and can be seen originating from the external aspect of the maxilla, the pterygomandibular raphe and the external aspect of the (edentulous) mandible.

Item no. MP1665

Head and Neck

This 3D printed specimen of a parasagittally sectioned head and neck demonstrates a range of anatomical features: Lateral aspect of the face: A window has been created to expose the parotid region. The pinna of the ear has been left intact, however the mastoid process has been exposed by reflection of the sternocleidomastoid (SCM) muscle. The parotid gland has been carefully removed to display structures which are normally embedded or hidden by the gland. The attachment of the posterior belly of digastric arising from the digastric groove medial to the mastoid process can be clearly seen.

Item no. MP1660

Superior Orbit

This 3D printed model captures a dissection in which the calvaria and cerebrum have been removed to expose the floors of the anterior and middle cranial fossae. The midbrain has been sectioned at the level of the tentorium cerebelli and on the cross sectional surface one can identify the superior colliculi, cerebral peduncles and the substantia nigra. Anterior to the mid-brain the vertebral artery can be clearly identified rising from the posterior cranial fossa and dividing into the posterior cerebral arteries.

Item no. MP1675

Medial Orbit

This 3D print displays the orbital contents and its close relations as viewed from the medial perspective when the majority of the lateral wall of the nasal cavity and the intervening ethmoidal sinuses have been removed. The posterior ethmoidal nerve (PEN) (a branch of the nasociliary nerve, CN V1) can be seen passing between the medial rectus (MR) inferiorly and the superior oblique muscle superiorly. Detailed anatomical description on request.

Item no. MP1685

Lateral Orbit

This 3D printed specimen shows the orbit from the lateral perspective when the bony lateral wall and part of the calvaria of the skull have been removed. The frontal and temporal lobes of the brain are exposed. In the orbit the lateral rectus (LR) has been divided to demonstrate the intraconal space. The muscle near its insertion has been reflected anteriorly to reveal the insertion of inferior oblique muscle (IO). The portion near its origin from the annulus is reflected to reveal the abducens nerve (VI Nv) entering the bulbar aspect of the muscle belly.

Item no. MP1680

Paranasal Sinus model

This unique model has been created from CT imaging and segmentation of the internal spaces of the viscerocranium. Parts of the skull have been retained but sections or windows have been removed to expose the paranasal sinuses. The paired frontal sinuses, with the right being partially subdivided, are coloured blue.

Item no. MP1630

Temporal Bone Model

Set of 3

This 3 part 3D printed model derived from CT data highlights the complex anatomy of the temporal bone including bone ossicles, canals, chambers, foramina and air spaces. In addition, the spatial relations between temporal bone and other structures of otological importance, i.e. carotid artery, dural venous sinuses, related nerves and the dura mater are indicated. Internal casts (endocasts) of the bony chambers and canals have been created to aid visualisation of the internal anatomy of the temporal bone. The model set consists of three parts: Part 1 Skull Preparation. Part 2 The Petrous Part Of The Temporal Bone. Part 3 The Auditory And Vestibular Apparatus.

Item no. MP1620

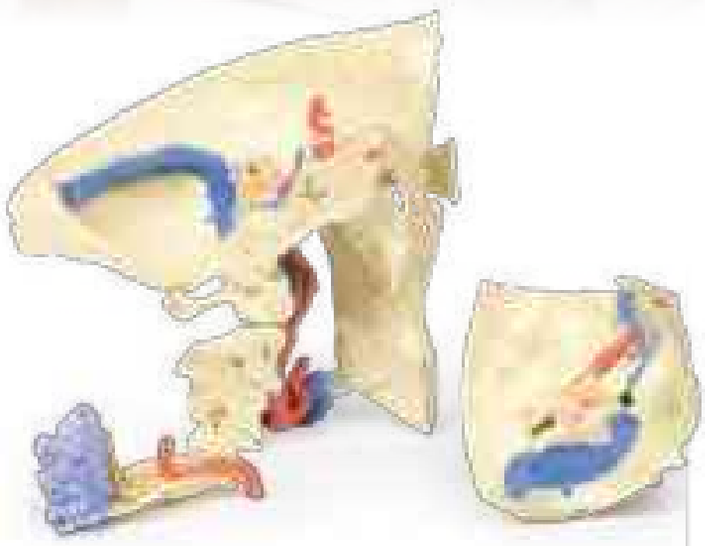

Circle of Willis

This 3D printed specimen demonstrates the intracranial arteries that supply the brain relative to the inferior portions of the viscero- and neurocranium. This print was created by careful segmentation of angiographic data. The model shows the paired vertebral arteries entering the cranial cavity through the foramen magnum and uniting to form the basilar artery. The basilar can be seen dividing into their terminal posterior cerebral arteries. The superior cerebellar arteries arise just proximal to this termination.

Item no. MP1600

Dural Skull

BEST SELLER

This 3D print of a dissected and opened cranial cavity displays the dural folds and dural venous sinuses, including the falx cerebri (preserved by a retained midsagittal portion of the calvaria. The intact tentorium cerebelli demonstrates the tentorial notch which normally houses the midbrain.

Item no. MP1610

Arterial and Venous Circulation

This 3D print integrates segmented angiographic data of both the cranial arterial and venous circulation into a single model. This model is a combination of 'Circle of Willis' MP1600, 'Cranial Arterial Circulation' MP1650 and 'Cranial Venous Circulation' MP1645 prints.

Item no. MP1640

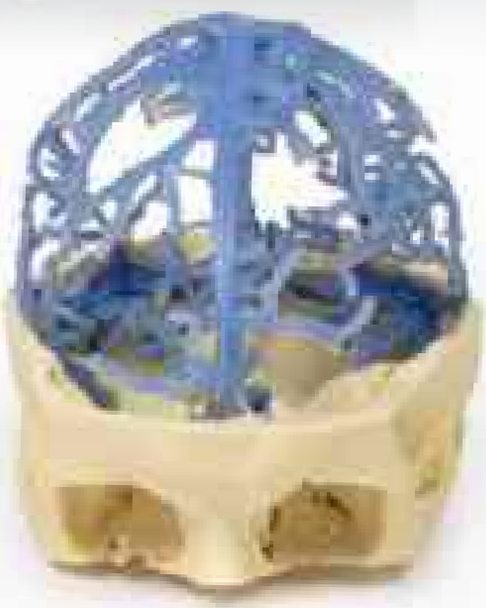

Venous Circulation

Based on the same dataset as MP1600 and MP1650, in this 3D print the dural venous sinus network has been segmented based on structures visible from the circulation of contrast medium. As a result, while most of the sinuses are present, the lack of contrast in the anterior portions of the venous system means that some structures (cavernous sinus, petrosal sinuses) are not included in the model. The extensive network of dural veins and venous lacunae are visible, joined in the midline to the superior sagittal sinus. Deep to this network of sinus veins are the great cerebral vein, the inferior sagittal sinus and the straight sinus to its convergence with the superior sagittal at the confluence of sinuses. Several dural veins drain into the left and right transverse sinuses as they pass anterior towards the petrous portion of the temporal bone. The sigmoid sinuses can be seen in the posterior cranial fossa prior to exiting the skull at the jugular foramen and forming the internal jugular vein (visible on the inferior surface of the skull).

Item no. MP1645

Arterial Circulation

Like our circle of Willis print, this model demonstrates the internal carotid and vertebral arteries entering the skull, branching into the intracranial arteries that supply the brain. This more expanded 3D print of the internal carotid and vertebral artery anastomoses and branches, inclusive of the circle of Willis, displays the full branching pattern of the cerebral and cerebellar arteries.

Item no. MP1650

Brain Steam

This 3D model preserves the several deep cerebral and diencephalic structures through to the proximal medulla oblongata and compliment the other isolated brainstem (BRW10) in our series. Superiorly, on the right side of the 3D model, the lentiform (lenticular) nucleus is in place and the corona radiata of the internal capsule is seen emerging around it. On the left, the lentiform nucleus is absent, but the caudate nucleus head and body are present medially on both sides.

Item no. MP1100

Brain Steam

This 3D model provides a view of the isolated brainstem anatomy from the midbrain to the medulla oblongata, and compliments the other diencephalon/brainstem 3D model (BR 10) in our series. Rostrally, the 3D model has been sectioned at an angle from the overlying diencephalon while retaining the mamillary bodies of the hypothalamus between the cerebral peduncles (anteriorly) and the pineal gland/epithalamus (posteriorly).

Item no. MP1101

Brain (Hemisection)

This 3D model is a midsagittal hemisection through a whole brain, preserving the right side anatomy and deep brain structures and spaces visible in the midline. In lateral view, the right cerebral and cerebellar hemispheres are covered in the arachnoid mater. In the midline view, the brain regions from the cerebrum to the medulla oblongata are preserved.

Item no. MP1102

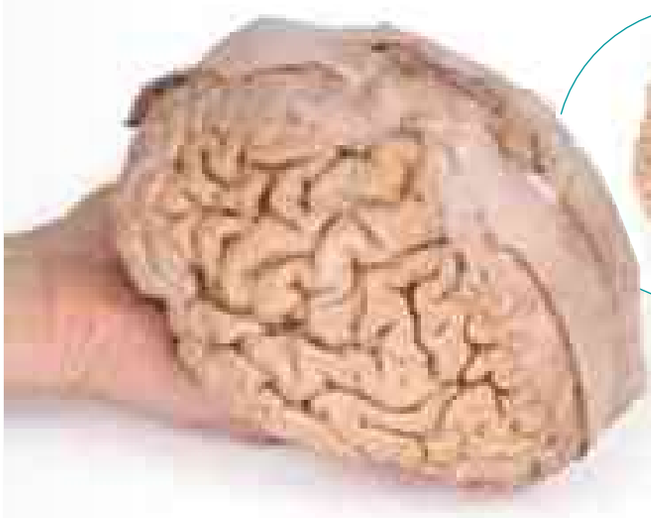

Brain (Cerebrum)

This 3D model provides a unique perspective on the anatomy of the cerebrum relative to the meninges. The cerebrum has been separated from the brainstem and cerebellum, with only parts of the midbrain and cerebral peduncles visible on the inferior surface. Adjacent to the cut section the olfactory tracts and bulbs can be seen extending along the inferior margin of the frontal lobes of the cerebrum.

Item no. MP1103

Sagittal Section of Head with Infratemporal Fossa Dissection

This 3D model provides a combined midsagittal section through the head and superior neck coupled with a deep dissection into the infratemporal fossa region and superficial dissection of the scalp.

Item no. MP1104

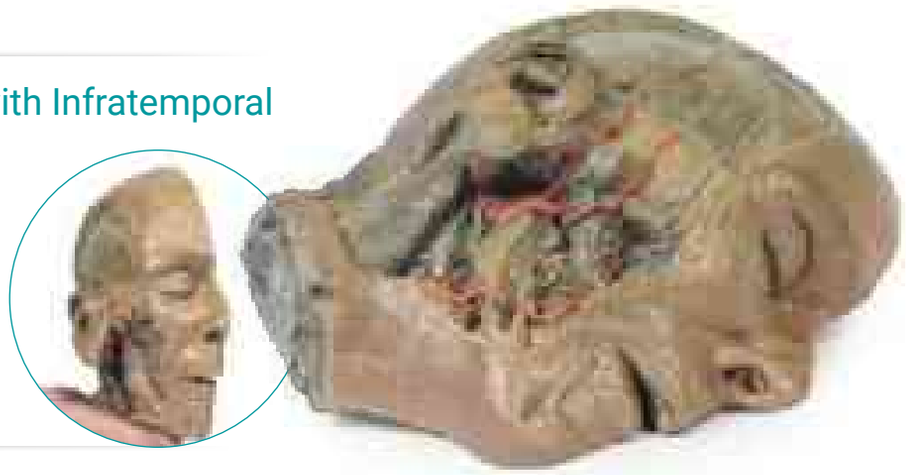

Median section trough head Sagittal Section of the Head with Deep Dissection

This 3D model combines a midsagittal section of the head with preservation of brain and cranial cavity anatomy, with a unique deep dissection of the pharyngeal region via removal of basicranial bone and the anterior parts of the atlas and axis. As the opposing side is undissected it has been digitally eliminated from the model.

Item no. MP1105

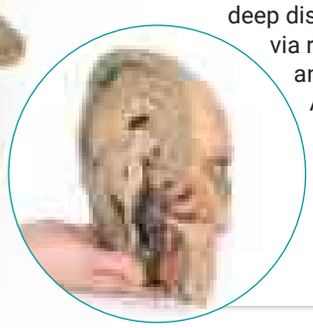

Sinus Pathways

This 3D model provides a midsagittal to parasagittal segment of a right head to demonstrate the relationships and passageways of the paranasal sinuses. These passageways have been highlighted with thin coloured markers to indicate the relationship of these communicating routes between the paranasal sinuses and the nasal cavity.

Item no. MP1106

Parasagittal Section of the Head and Neck

This 3D model of the head and neck represents a specimen sectioned just off the midsagittal plane to retain some midline anatomical structures (e.g., the falx cerebri, the septum pellucidum, the nasal septum) that are absent from other specimens in the series. There has also been fixative-induced shrinkage of the neural tissue. This reduction in volume has the benefit of exaggerating the space between the brain and endocranial contours and structures which are normally in closer approximation. The undissected side of the specimen has been digitally removed.

Item no. MP1107

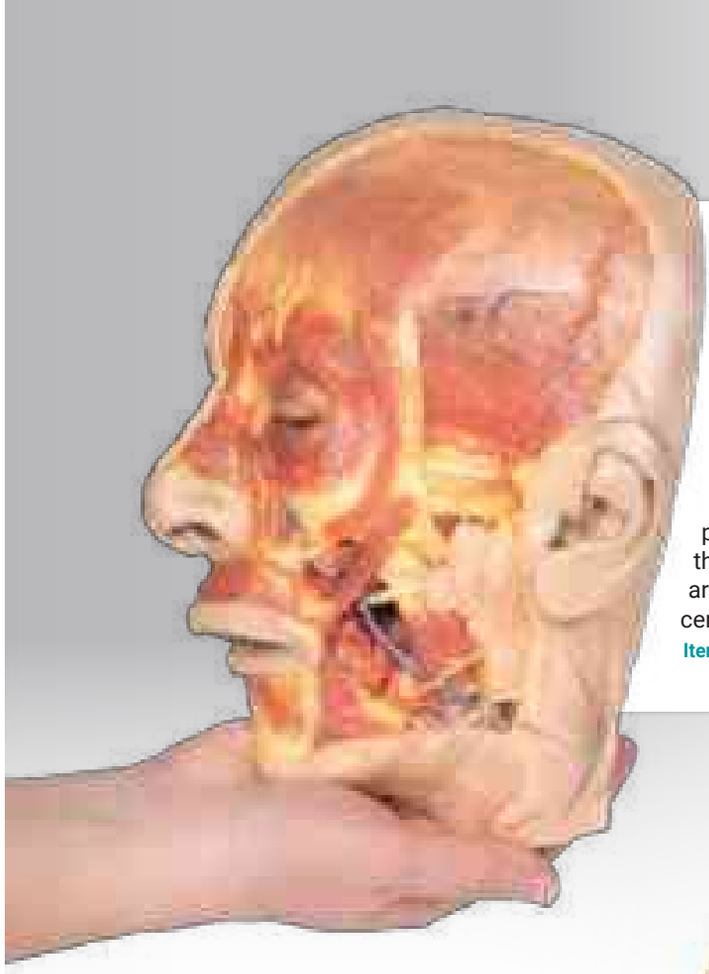

Superficial Face

This 3D model presents a superficial dissection of a left face anterior to the ear with false colouring highlighting a series of neurovascular structures alongside the superficial muscles of facial expression. This compliments the more expanded superficial dissection of the face and lateral head presented in our HW 45 model. The undissected regions of the model have been digitally removed. Starting just anterior to the ear, the opened window of dissection has exposed the parotid gland and associated duct transmitting anterior towards the oral cavity. Exiting from the margins of the parotid gland are terminal branches of the facial nerve (CN VII), including the cervical, mandibular, buccal, zygomatic and temporal.

Item no. MP1108

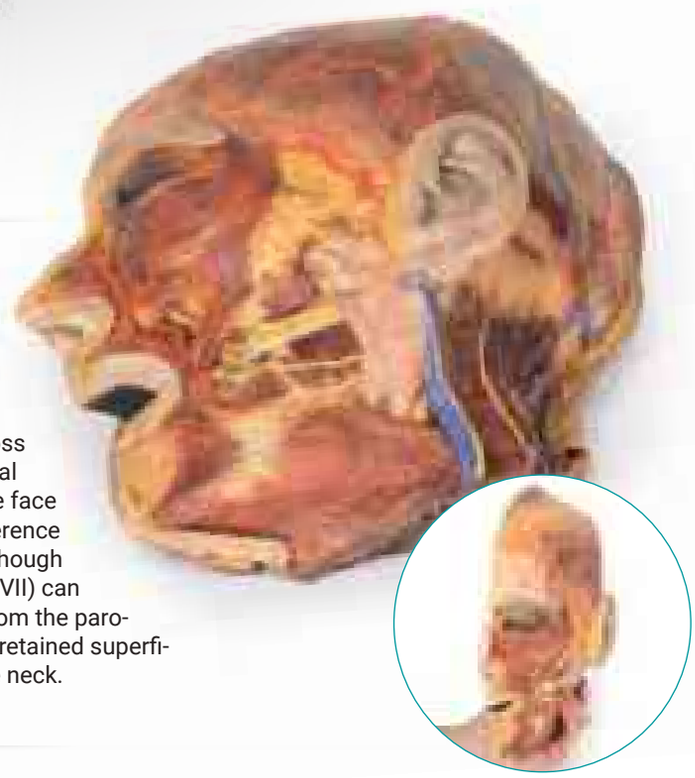

Superficial Facial nerves + Parotid Gland

This 3D model presents the superficial anatomy of the face and head, and compliments the superficial facial anatomy of our HW 44 model with a more expanded dissection across the scalp and occipital regions. The superficial neurovascular and muscular structures in the face largely mirror the structures described in reference to our HW 44 specimen (see description), although the terminal branches of the facial nerve (CNVII) can be largely followed across a longer course from the parotid gland and the platysma muscle has been retained superficial to the mandible and extends towards the neck.

Item no. MP1109

Transverse Section of the Head

This 3D model preserves a transverse section through the cranial cavity with partial dissection of the brain and exposure of the left orbital roof, alonside a deep dissection of the face and temporomandibular joint region. Within the cranial cavity, the dura mater has been largely removed from the anterior cranial fossa, with retention of the layer in part across the middle and posterior cranial fossae.

Item no. MP1110

Sagittal Section of Head and Neck with Infratemporal Fossa and Carotid Sheath Dissection

This 3D model provides a complimentary specimen to the H 11 and H 12 head and neck specimens by providing a perspective of the endocranial cavity without the brain, and a lateral dissection inclusive of neck anatomy. In the midsagittal section, the removal of the brain (and reflection of the medulla oblongata inferiorly) affords a full view of the dura mater lining the endocranial cavity, including the tentorium cerebelli spanning from the transverse sinus to the attachment to the clinoid process of the sphenoid.

Item no. MP1111

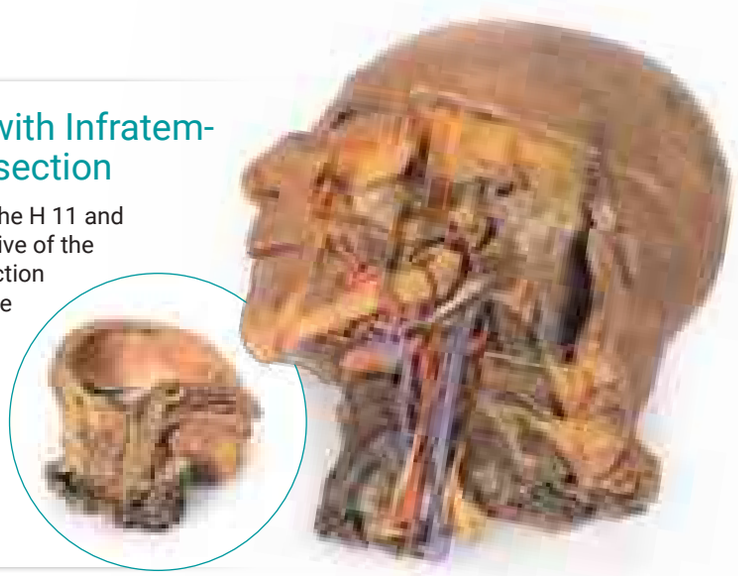

Parotid Gland and Facial Nerve Dissection

This 3D model provides a superficial dissection window into the lateral face to demonstrate the anatomy of the parotid gland relative to surface features and neurovascular structures. These structures are of particular significance for management in Mohs surgery in the management of skin cancers, or in certain plastic and reconstructive surgical procedures.

Item no. MP1112

Thoracic cross section at T6

This model is a cross-section of the thorax at the level of the T6 vertebra. Beginning posteromedially at the spinal cord within the vertebral canal, then moving radially, the costovertebral joints of the 6th ribs are visible, followed by several other ribs around the margin of the thoracic cavity, a pair of which unite anteriorly with the sternum via the costosternal joints. Additionally, the oesophagus and descending aorta are visible anterior and lateral to the T6 vertebral body, respectively.

Item no. MP1120

Pericardial Space

In this specimen the heart itself has been removed to demonstrate the reflections of parietal peritoneum and the orientation of the heart relative to other structures, including the diaphragm (diaphragmatic surface) and the lungs (left and right pulmonary surfaces). The pericardium is the multilayered fibroserous sac that encloses the heart and is continuous with the serous visceral pericardium (epicardium) of the heart itself. In normal anatomical position, the boundaries of the parietal pericardium are also the boundaries of the middle mediastinum (what we call coterminous).

Item no. MP1121

Thorax with Heart and Vessels

The superior thoracic aperture contains structures emerging from the thorax and entering the head and neck and upper limb. In this specimen, both clavicles, key venous structures and other musculature have been removed. Despite this, other important components of anatomy can be observed. Key structures include the Trachea seen most superiorly with a thick ring of cartilage, rib one has been exposed prior to meeting its costal cartilage, travelling in a lateral to medial direction and the anterior scalene muscle inserting into Rib one superiorly.

Item no. MP1122

Heart

This 3D model represents a ‘normal’ sized adult heart with light dissection to the epicardium to expose the coronary arteries and cardiac veins. At the base of the heart, the terminal part of the superior vena cava and azygous vein can be observed just prior to draining into the right atrium. Immediately adjacent to the superior vena cava, the arch of the aorta has been preserved with the origins of the aortic arch derivative arteries.

Item no. MP1123

Male Hemipelvis and Thigh

This 3D model preserves a right male pelvis sectioned just superior to the L5 vertebra and sectioned at the midsagittal plane, with the thigh preserved to near the midshaft of the femur. This specimen compliments our LW 91 female hemipelvic specimen and thigh. The common iliac artery is preserved with several key branches visible, particularly the distribution of the internal iliac within the true pelvis.

Item no. MP1142

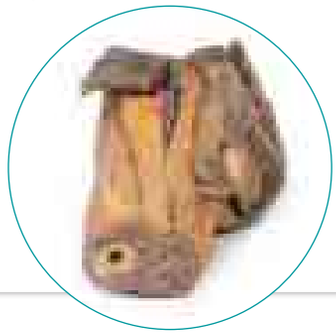

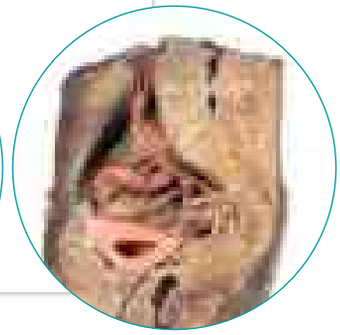

Hilum of the Left Lung

The hilum of a lung is the point at which visceral and parietal pleura meet and functions with the pulmonary ligament as the lungs only connection with the rest of the body. This connection includes the Pulmonary Artery, Superior and Inferior Pulmonary Veins, Main Bronchi, Nerves and Lymphatics. As the definition of an artery involves carrying blood AWAY from the heart, this will be deoxygenated blood in the pulmonary system, in contrast with the systemic circulation. Similarly, veins carry blood TOWARDS the heart, meaning it will be oxygenated in the pulmonary system.

Item no. MP1124

Hilum of the Right Lung

The hilum of a lung is the point at which visceral and parietal pleura meet and functions with the pulmonary ligament as the lungs only connection with the rest of the body. This connection includes the Pulmonary Artery, Superior and Inferior Pulmonary Veins, Main Bronchi, Nerves and Lymphatics.

Item no. MP1127

Lung Slab, Hilum Removed

The lung has been dissected following a parasagittal plane, removing the mediastinal surface. Ordinarily, the pulmonary arteries, veins and bronchi can be observed entering the lung in the hilum – but the primary bronchi cannot be seen in this specimen as they have already divided substantially. It is unclear how far laterally the specimen has been dissected hence the bronchi subdivision level (secondary or tertiary) cannot be determined.

Item no. MP1125

Right Lung, Hilum Removed

This 3D model represents the complimentary section to the TW 63 right lung hilum 3D model within our series and provide a direct contrast to the TW 61 left lung section. While expressing few discrete features, this 3D model affords a view of the major structural elements of the right lung from the apex to the base. On the lateral aspect, the well-developed oblique and horizontal fissures divide the lung into its three lobes (superior, middle, inferior) – and the cross-section demonstrates the depth of these fissures into the deep portions of the organ itself.

Item no. MP1126

Abdomen with Bilateral Hernias

This 3D model represents one of the largest and most complex in the series, consisting of a partial torso from the diaphragm to the proximal thigh with a complete abdominal cavity preserving varying levels of dissection. This 3D model also records the rare, simultaneous occurrence of indirect and direct inguinal hernias allowing for a consideration of the anatomical underpinnings for both conditions. Given the scale of the dissection this 3D model description is divided into discrete parts based on views and regions. The diaphragm: on the superior aspect of the model the diaphragm is preserved, and while slightly distorted due to removal of the thoracic ribs through dissection, both domes and costodiaphragmatic recesses can be appreciated. The fibrous pericardium is present on the superior surface of the central tendon, with the terminal part of the inferior vena cava visible in the caval foramen. Just lateral to caval foramen is the oesophagus within the oesophageal hiatus, and then the descending thoracic aorta approaching the aortic hiatus just ventral to the thoracic vertebrae.

Item no. MP1130

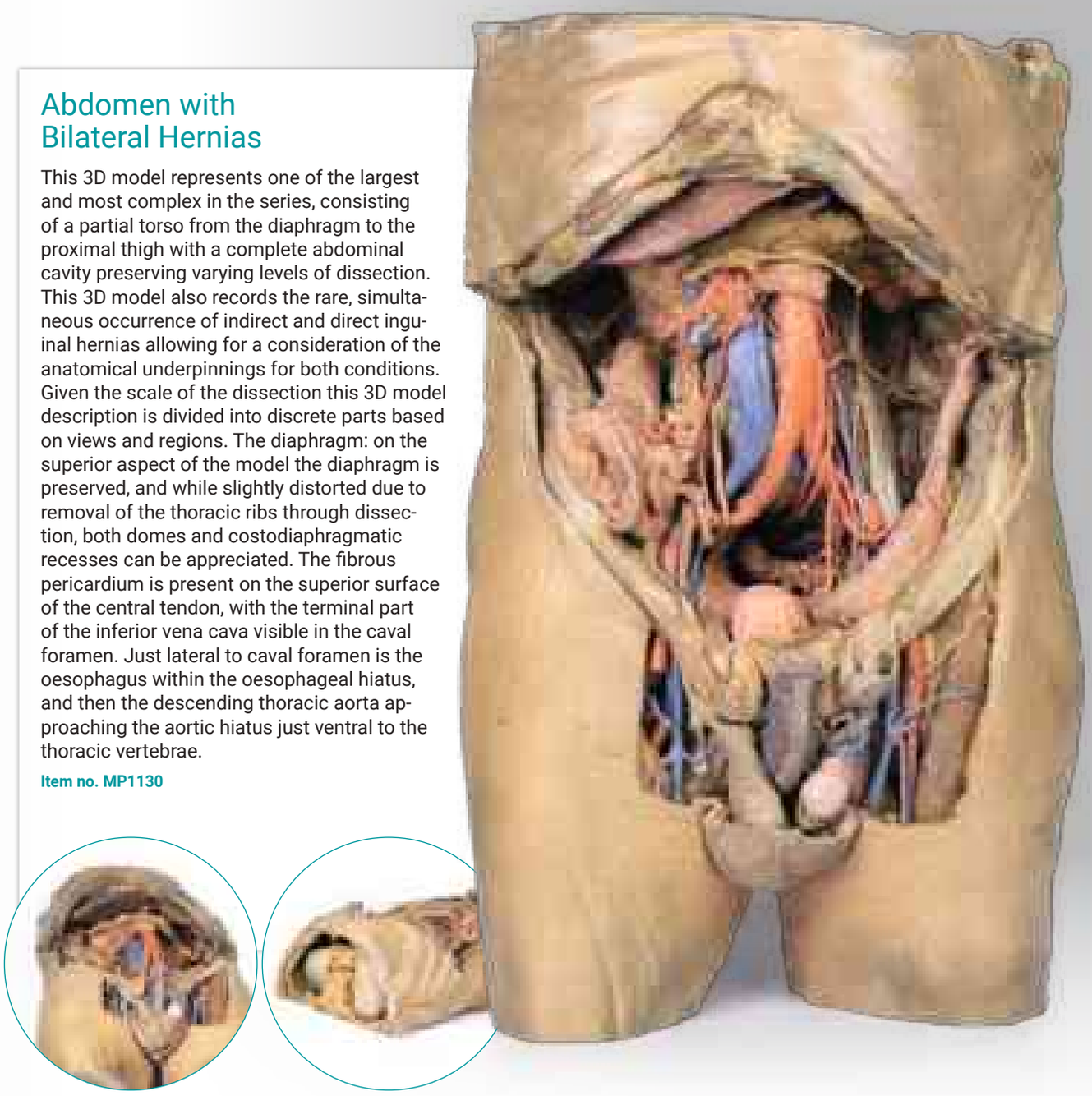

Abdomen Vasculature

Coeliac Trunk: Supplying the embryological foregut, the celiac trunk arises from T12 spinal level. Branches that can be observed in this specimen include the Left gastric artery arising from the left portion of the celiac trunk; remains of the splenic artery arising from the celiac trunk and visible passing to the left hypochondrium; the Common hepatic artery, located to the right of the celiac trunk and giving off key branches; the Gastroduodenal artery, branching inferior to into the right gastric artery, and provide an anastomosis to the superior mesentery artery via the superior pancreaticoduodenal and the Proper hepatic artery, beginning after the gastroduodenal artery, branching to form the Left hepatic artery, the first branch of the proper hepatic artery, Right hepatic artery, located inferiorly, eventually giving rise to the Cystic artery, connecting to the gallbladder.

Item no. MP1131

Vasculature of the Spleen

At the splenic hilum, the splenic artery and vein can be seen entering the spleen to supply and drain the organ. The opening of the splenic vein has been kept patent by the insertion of silicon tubing in the model. This model shows the most superior branch of the splenic vein has been sectioned from its normal passage into the spleen. The “tortuous” of twisted shape of the splenic artery can be appreciated as it branches at the hilum. This reflects the overall curled and twisted shape of the vessel across its course from the coeliac trunk to the spleen.

Item no. MP1132

Abdomen with Inguinal Hernia

Diaphragm and Xyphoid Process: The diaphragm has been secured to the superior border of the dissected specimen with sutures to ensure an unobstructed view of the abdomen. The xyphoid process is in the middle of this sutured border. Liver and Gallbladder: The liver in the right hypochondrium has been pushed laterally to reveal the kidney posterior to it. The falciform ligament divides the right and left anatomical lobes of the liver and enveloping ligamentum teres, which is a remnant of the umbilical vein which is present during foetal development. Below ligamentum teres at the inferior border of the liver in this model, the gall bladder is sandwiched between the anatomical lobes of the liver.

Item no. MP1133

Stomach

This 3D model is an isolated stomach with two dissection windows to expose the rugae and pylorus. A small portion of the terminal oesophagus is preserved at the cardiac region, and a small portion of the proximal duodenum beyond the pyloric sphincter. The large window within the body of the stomach allows for a clear view into the fundus and the welldeveloped rugae on the posterior aspect of the wall of the organ. The smaller window, opened just at the pyloric region, allows for an appreciation of the thickening of the organ wall at the pyloric sphincter just proximal to the start of the duodenum.

Item no. MP1134

Spleen and Pancreas

This 3D model preserves the deep foregut organs: the descending, horizontal and ascending duodenum, the pancreas, and the spleen. A small window in the duodenum has been opened to allow for a view of the plicae circularis within this proximal part of the small intestine (and contrasts the strong rugae development seen in the stomach; see AW 42).

Item no. MP1135

Liver with Vessels and Gall Bladder

The size and shape of this specimen varies somewhat from a typical liver. It is less wedge-shaped and longer in the superoinferior dimension (on the posterior view this would translate to a greater vertical height). Normally, a liver is less than 16cm in the midclavicular line.1 This specimen measures approximately 18cm in the midclavicular line, suggesting some degree of hepatomegaly.

Item no. MP1136

Internal Abdominal wall

This 3D model captures the internal surface of the anterior abdominal wall, a region oftentimes removed or damaged during dissection (and complimenting our A8 abdominal specimen where the anterior wall has been removed). The parietal peritoneum has been removed from the internal surface of the specimen in order to more clearly demonstrate the relationships of the anterior abdominal muscle fibres and connective tissue structures as they converge on the midline.

Item no. MP1137

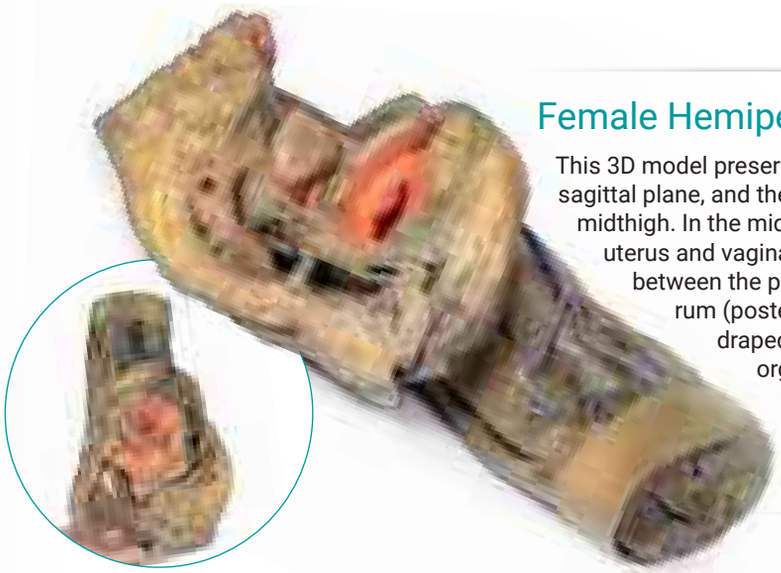

Female Hemipelvis and Thigh

This 3D model preserves a left pelvis divided at the midsagittal plane, and the proximal thigh to approximately the midthigh. In the midsagittal section, the urinary bladder, uterus and vagina, and rectum can be seen in sequence between the pubic symphysis (anteriorly) and the sacrum (posteriorly). The retention of the peritoneum draped across the superior surface of these organs allows for view of the vesicouterine and rectouterine pouches.

Item no. MP1140

Female Pelvis Deep Dissection

This 3D model presents a deep dissection and isolation of the pelvis from surrounding regions, particularly demonstrating visceral and neurovascular structures relative to deep ligaments and osseous features. Within the false pelvis, the sigmoid colon descends on the left side of the specimen to the rectum, passing superficially across the pelvic brim and the passage of the common and external iliac artery and vein.

Item no. MP1141

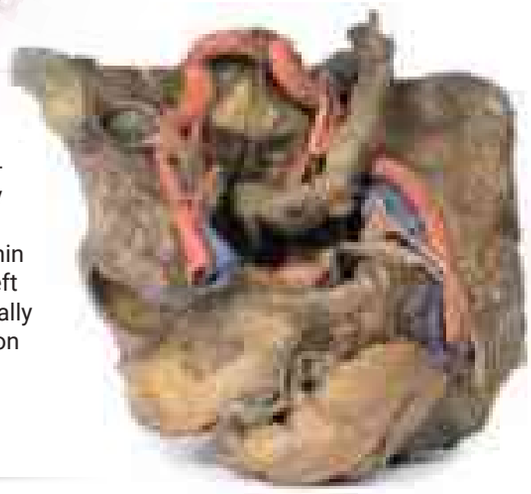

2.0 Pathology
Rare Pathology cases

Berry Aneurism of Basilar Artery

This brain has been sliced in the mid-sagittal plane. It comprises a whole hemi-section of the brain about 1cm thick. On the medial surface a large darkly-coloured ovoid berry aneurysm measuring 5 x 2 cm in diameter, arising from the basilar artery is clearly visible. It has eroded up into the midbrain, compressing the third ventricle from below, and inferiorly into the substance of the pons. The wall of the aneurysm appears intact although blood clot is seen in the third ventricle and appears to be leaking through the lateral wall of that ventricle.

Item no. MP2001

Cerebral Haemorrhage

The left hemisphere of the brain has been sliced in the parasagittal plane, and the cut surface displays a large cerebral haemorrhage in the parietal and frontal lobe. The haemorrhage and associated clot are causing extensive distortion of the left external capsule and lateral ventricle. The source of the bleeding was a ruptured aneurysm of the left middle cerebral artery.

Item no. MP2002

Glioma grade 3-4, causing papilloedema

The specimen shows a large intracerebral lesion, which has obliterated the lateral ventricles and the inner 2/3 of the internal capsule and basal ganglia on the right side. It is infiltrating across the corpus callosum and distorting the aqueduct. The tumour is fairly well demarcated and vascular with numerous areas of haemorrhage and necrosis, causing its mottled variegated appearance.

Item no. MP2003

Meningioma

between the two frontal lobes. The tumour is compressing the frontal lobes. It has a pinkish cut surface with some yellow areas indicating necrosis. It was attached to the dura mater anteriorly. This is an example of a meningioma.

Item no. MP2004

Left cerebral infarct

A coronal section of the cerebral hemispheres shows irregular cystic cavities in the territory of distribution of the right middle cerebral artery. The cavities of the infarct have irregular, yellow walls and show partial collapse. There is compensatory dilatation of the left lateral ventricle. On the posterior aspect, the arteries below the mammillary bodies were moderately atheromatous, although this is difficult to visualise macroscopically.

Item no. MP2005

Pituitary Adenoma

The brain specimen is sliced in the sagittal plane to the right of the falx cerebri, which remains in-situ. The pituitary gland has been completely replaced by a round tumour 4cm in maximum diameter. The tumour cut surface is pale brown and homogenous (except for an area of haemorrhage superiorly, likely caused by surgical trauma). The tumour has resulted in upward displacement of the midbrain. Tumour erosion has destroyed the sphenoid bone; thus, the sella turcica is enlarged (arrow). The optic chiasma is compressed by the tumour. Histologically, this tumour was a chromophobe adenoma arising from the anterior pituitary.

Item no. MP2006

Metastatic Adenocarcinoma in the Brain

This brain specimen is cut in the coronal plane. A circumscribed, variegated, pink-grey tumour is evident in the right frontal lobe. The tumour is involving the grey and white matter. Compression of the right lateral ventricle by the lesion is apparent with shift of the midline structures also seen.

Item no. MP2007

Ventriculitis, Secondary to Septicaemia

This specimen is an example of ventriculitis, with pneumococcal meningitis and right basal pneumonia also being found at autopsy. The horizontal slice through both cerebral hemispheres displays both of the lateral ventricles. The ventricles show a thickened, rough ependymal lining with cellular debris accumulation around the choroid plexus and also in the anterior horn. The lower surface shows similar changes and also displays the normal arrangement of the caudate nucleus, lentiform nucleus and internal capsule.

Item no. MP2008

Cerebral Haemorrhage, secondary to Acute Myeloid Leukaemia (AML)

The specimen is a horizontal slice of brain displaying the superior cut surface. In the right frontal and parietal regions are two large intraparenchymal haemorrhages each 5 cm in maximum diameter. Several smaller haemorrhages are present in the white matter of both hemispheres. This is an example of multiple intraparenchymal cerebral haemorrhages in a patient with acute myeloid leukaemia (AML).of vascular lumen and involvement of the blood vessel walls. The inflammation extended into the cerebral parenchyma causing haemorrhage and necrosis.

Item no. MP2009

Cerebral Arterio-Venous Malformation

The specimen is a coronal slice of the brain that passes through the parietal lobes. Cortex and white matter on the medial aspect of the right cerebral hemisphere have been replaced by a mass of abnormal tissue 4 cm in greatest diameter. This lesion extends from the superior surface down to the roof of the lateral ventricle. A closer inspection reveals the tissue to be a network of tortuous vascular channels and intervening tissue.

Item no. MP2010

Intracranial space-occupying lesion

The specimen is a coronal section of a brain. It is evident that the brain has been compressed laterally and downwards by a right-sided expanding intracranial mass, probably a meningioma. The original mass is not present. The anterior face shows shift of midline structures with subfalcine herniation* of the cingulate gyrus. The posterior face (see photo) shows haemorrhage of varying ages within the temporal lobe and the pons, typical of supratentorial mass lesions. There is also ventricular asymmetry.

Item no. MP2011

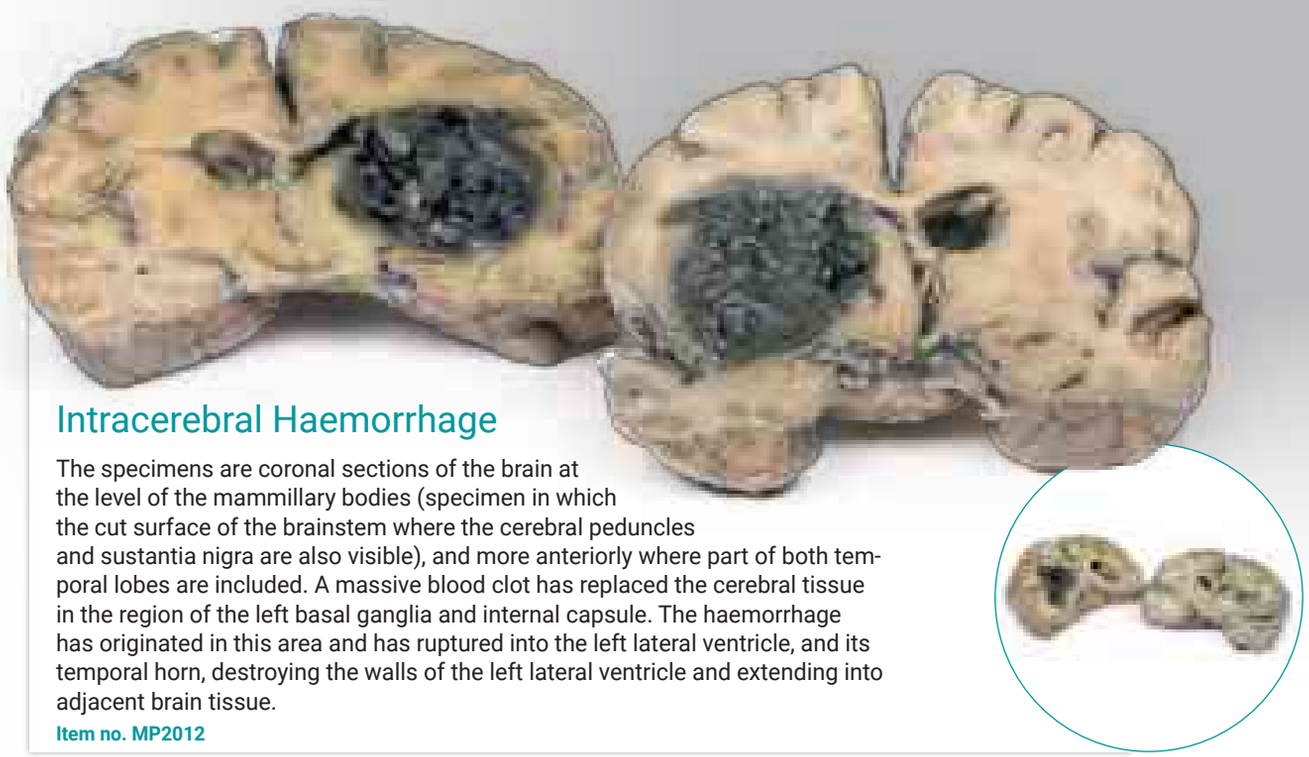

Intracerebral Haemorrhage

The specimens are coronal sections of the brain at the level of the mammillary bodies (specimen in which the cut surface of the brainstem where the cerebral peduncles and sustantia nigra are also visible), and more anteriorly where part of both temporal lobes are included. A massive blood clot has replaced the cerebral tissue in the region of the left basal ganglia and internal capsule. The haemorrhage has originated in this area and has ruptured into the left lateral ventricle, and its temporal horn, destroying the walls of the left lateral ventricle and extending into adjacent brain tissue.

Item no. MP2012

Ruptured Berry Aneurysm

The specimen shows the basal surface of the brain. There is a saccular aneurism 5 mm in diameter at the junction of the right internal carotid and the posterior communicating artery, which has ruptured. There is subarachnoid blood in the immediate area in the cisterna magna and on the inferior surface of the right frontal lobe. There is a similar unruptured aneurysm on the left side. The right frontal lobe appears softer and more friable anteriorly.

Item no. MP2013

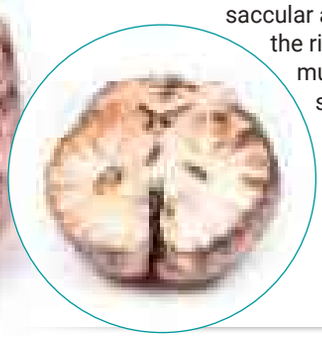

Astrocytoma

This brain specimen is a coronal section. In the right temporal lobe, a poorly demarcated tumour is present. There is enlargement of the hemispheres and flattening of the gyral pattern. From the posterior aspect of the specimen subfalcine herniation* is appreciated and the tumour appear less well differentiated with haemorrhagic and necrotic foci. Histology of this tumour showed an astrocytoma, Grade III/IV.

Item no. MP2014

Glioblastoma multiforme

Coronal section through the cerebral hemisphere demonstrates a round, haemorrhagic, variegated tumour in the left temporal lobe. Less well-defined tumour tissue extends across the mid-line replacing the corpus callosum. The ventricular system has been almost totally obliterated. Further sections through the cerebral hemisphere confirmed that these apparently separate lesions are extensions of one massive tumour.

Item no. MP2015

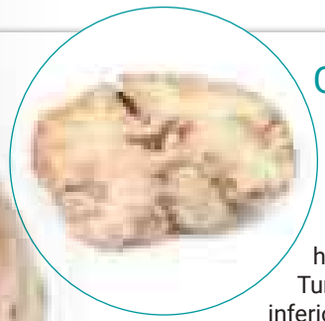

Glioblastoma multiforme

Coronal sections of the brain post mortem show a 4cm necrotic and haemorrhagic tumour. Tumour invasion from the inferior frontal lobe into the lateral ventricle is apparent. Meningeal spread is evident on examination of the posterior aspect of the specimen.

Item no. MP2016

Craniopharyngioma

The brain has been sectioned in the sagittal plane, displaying the medial surface. A pink-grey, ovoid tumour measuring 2.5 x 1.5 cm on the cut surface is centred in the region of the hypothalamus. It is encapsulated except at its ventral pole where tissue has been removed at previous surgery, and the cut surface reveals a microcystic or spongy appearance. The tumour distorts the 3rd ventricle and extends to obliterate the Foramen of Munro. The optic chiasm is displaced caudally (arrow).

Item no. MP2017

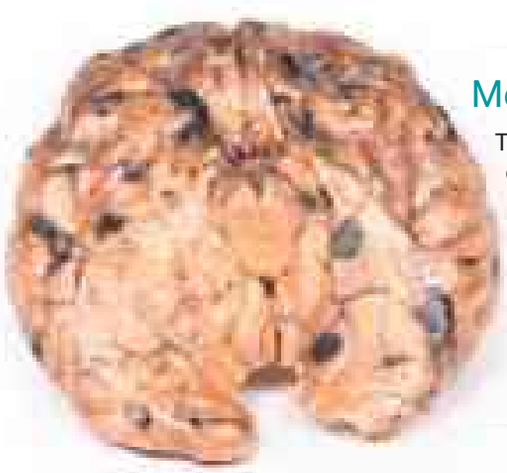

Metastatic melanoma

This specimen demonstrates widespread intracerebral melanoma metastases. The inferior surface is characterised by many elevated dark nodules up to 1.5 cm in diameter. Similar lesions are present on the cut superior surface where it is seen that these secondary melanotic deposits are confined exclusively to the grey matter. The tumour deposits are not encapsulated and are invading the cortex. Some necrosis and haemorrhage is present.

Item no. MP2018

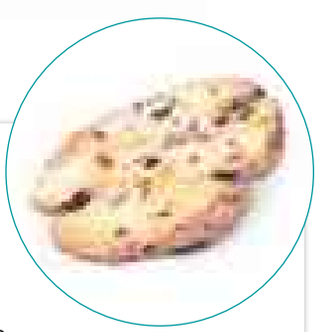

Metastatic carcinoma in the brain

The specimen is the cerebrum sliced horizontally. On the superior view, the right hemisphere is clearly enlarged, particularly in the parietal region where the gyrae are widened and 3 cystic tumours are evident. The largest, 5 cm in diameter, is in the right parietal region. A smaller tumour, 2 x 1.5 cm in diameter, is seen close to the posterior margin of the largest tumour. A third one, 1.5 cm in diameter, is present in the left parietal region.

Item no. MP2019

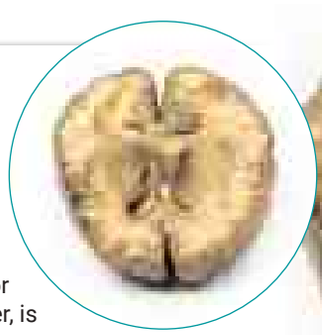

Abdominal Aortic Aneurysm (AAA)

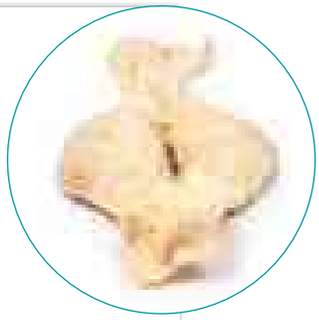

The specimen consists of lower abdominal segment of aorta together with common iliac vessels and proximal portions of the internal and external iliac arteries. A large 10 x 7 cm aneurysm is situated below the origin of the renal arteries extending to the aortic bifurcation. The aneurysm with its severe thinning of the wall of the abdominal aorta is partly lined by a laminated thrombus, indicating the chronicity of the process.

Item no. MP2030

Right Ventricular Hypertrophy (RVH)

The specimen is of the external surface of the heart viewed from the anterior aspect. The right ventricle is greatly enlarged and hypertrophied. All appears to be normal otherwise. This is an example of right ventricular hypertrophy (RVH) in a patient with emphysema.

Item no. MP2031

Atrial septal defect

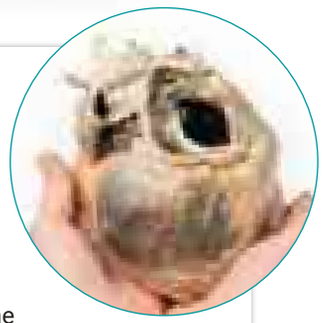

The heart is viewed from the left side. The left atrium has been opened to display a large ovoid defect 3.5 cm in greatest diameter in the interatrial septum. Only a small postero-inferior crescentic rim of septum remains. The left ventricle is small, and the right ventricle is hypertrophied (see posterior aspect of specimen where part of the right postero-lateral wall of the right ventricle has been cut away to demonstrate the thickened wall).

Item no. MP2032

Bicuspid Aortic Valve

The heart has been opened to display the left ventricle and associated valves. The aortic valve has 2 cusps instead of the usual three. The valves are otherwise normal apart from patchy slight thickening. The aortic origins of the left and right coronary arteries are widely patent, as is the left circumflex coronary artery, seen cut transversely in the atrio-ventricular groove at the right hand lower edge of the specimen.

Item no. MP2033

Congenital Pulmonary Stenosis

The specimen is the child's heart. View from the left side and note the pulmonary artery has been opened to display the upper surface of the pulmonary valve. This abnormal valve consists of a thickened conical diaphragm, with an opening 2 mm in diameter at the apex. The opened pulmonary artery has a large post-stenotic dilatation. There is right-sided cardiac enlargement due to marked dilatation of the right atrium and right auricle (opened), and right ventricular hypertrophy (the wall has been cut in two places [one penetrating, one one not] to expose the hypertrophied myocardium).

Item no. MP2034

Hydatid Disease Affecting the Heart and Aorta

The specimens are of the heart, with the left ventricle being laid open, and of the aorta at its common iliac bifurcation. The aorta shows some atheromatous depositions in the upper portion. There is a large mass of antemortem clot at the point of iliac bifurcation with extension down both common iliac arteries.The heart shows hypertrophy of the left ventricular wall, and an abnormal communication between the left ventricle and atrium running through the posterior cusp of the mitral valve via the papillary muscle into the left ventricular cavity.

Item no. MP2035

Hypertrophic Subaortic stenosis

This is a longitudinal section through the heart displaying the left and right ventricles and interventricular septum. The outstanding abnormality is a grossly thickened interventricular septum and left ventricular hypertrophy. The aortic cusps that are visible appear unremarkable, as does the mitral valve. The ventricular septum is so large that it encroaches on the lumen of the left ventricle.

Item no. MP2036

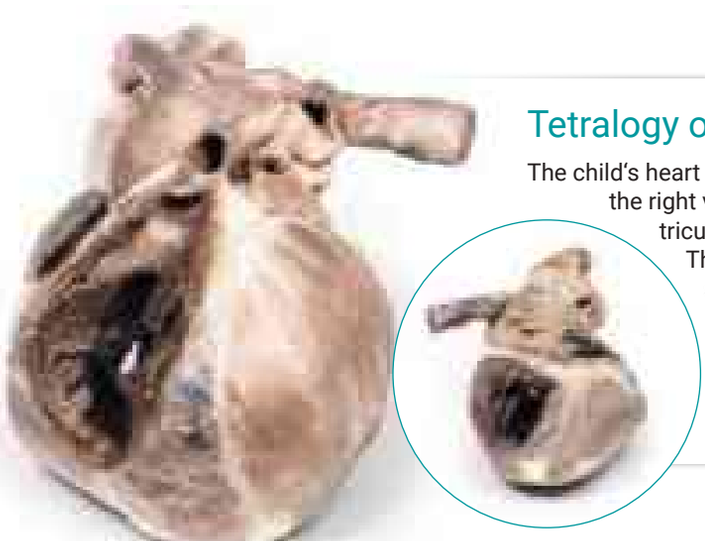

Tetralogy of Fallot

The child's heart is viewed from the anterior aspect. The anterior wall of the right ventricle has been excised to reveal prominent right ventricular hypertrophy and a narrowed pulmonary outflow tract. The pulmonary valve ring is also small, with a bicuspid stenosed valve. There is a patch of endocardial fibrosis in the outflow tract below the pulmonary valve. The origin of the aorta overlies a high ventricular septal defect.

Item no. MP2037

Rheumatic endocarditis

The specimen is that of a heart opened to show the left atrium and left ventricle. The mitral valve has been cut, but those visible parts show significant thickening. The left atrial wall shows deposition of blood and fibrin. The left auricular appendage is filled with blood clot, caused by atrial fibrillation. The mural thrombus on the atrial wall is in the typical site:- the deep layers of the endocardium forming irregular thickenings, called MacCallum's plaques (arrows).

Item no. MP2039

Calcified Aortic Valvular Stenosis Bicuspid Aortic Valve

The specimen is partial horizontal 1.5cm slice through the plane of the left atrium whose smooth internal lining together with the left auricular appendage and part of the left ventricle are visible on the inferior aspect. On the superior aspect the pulmonary trunk (and part of the pulmonary tricuspid valve) and aorta, including the affected abnormal bicuspid valve, are clearly discernible.

Item no. MP2038

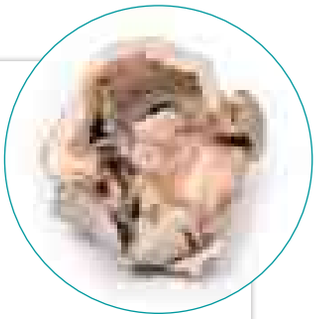

Traumatic Oesophageal-aortic fistula

The specimen is a block dissection of distal trachea (posterolateral on right margin), aortic arch (opened in coronal plane and viewed from anterior aspect) and oesophagus (posteriorly and opened longitudinally). The oesophageal mucosa is ulcerated and haemorrhagic. A small blue probe identifies a fistula between the oesophagus and posterior wall of the thoracic descending aorta.

Item no. MP2040

Acute Bacterial Endocarditis

This small heart displays the left ventricle and associated valves. The non-coronary cusp of the aortic valve is ulcerated and perforated and has friable vegetations attached. Immediately below this cusp a perforation extends into the right atrium just above the tricuspid valve (see back of specimen. The other aortic cusp is also thickened. This is an acute bacterial endocarditis with aortic cusp and atrioventricular perforations.

Item no. MP2041

Syphilitic Aneurysm

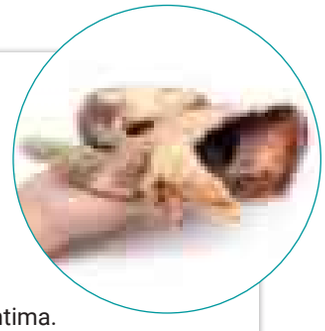

This specimen is the patient's enlarged heart, including the aortic arch and descending aorta. The ascending aorta is dilated up to 7 cm in diameter, and is expanded superiorly by a large aneurysmal bulge 11 x 13 cm in diameter. This has been opened to display the wrinkled scarred intimal surface. There is also marked atheroma of the intima. The innominate, left common carotid and subclavian arteries have been displaced towards the patients left by the aneurysm.

Item no. MP2042

Ruptured Thoracic Aortic Aneurysm

The heart displays both ventricles from the posterior aspect. There is a prominent saccular dilatation of the thoracic ascending aorta, which shows several atherosclerotic plaques and posteriorly is seen to be ruptured (identified by the dark staining). Both ventricles are hypertrophied. The coronary arteries together with the aortic and tricuspid valves are normal. This is an example of a ruptured aneurysm of the ascending aorta.

Item no. MP2043

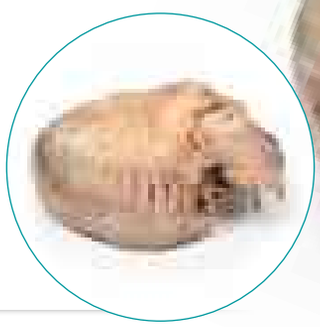

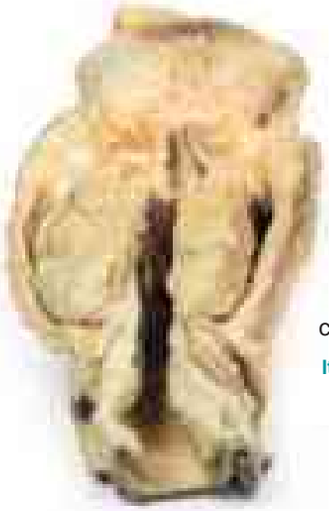

Carcinoma of Larynx

The specimen consists of tongue, pharynx, larynx, oesophagus and trachea and has been mounted in the coronal plane. The oesophagus and trachea have been opened from the posterior aspect. There is a 5 x 4 x 2 cm fungating carcinoma evident extending into both pyriform fossae. The surface of the tumour is irregular with shaggy areas of necrosis. The tumour has arisen from the larynx and involves both vocal cords, the left aryepiglottic fold and both pyriform fossae.

Item no. MP2050

Carcinoma of Pyriform Fossa

The specimen is the amputated larynx viewed from behind. It shows an irregular fungating tumour arising from the left pyriform fossa. There is distortion and oedema of the laryngeal tissues. Histologically, this was a squamous cell carcinoma.

Item no. MP2051

Carcinoma of Larynx

This is the patient's laryngectomy specimen. The larynx has been sliced open and is viewed from the posterior aspect. There is significant right vocal cord distortion by an irregular ulcerating tumour. Mucosal congestion is also noted. Histologically this was a well differentiated squamous cell carcinoma (SCC).

Item no. MP2052

Inhaled Foreign Body – trachea

This specimen shows the lower trachea and main bronchi. These have been cut open and the left upper lobe has been sliced to display the cut surface. At the point of origin of the left upper lobe bronchus there is an impacted foreign body; an inhaled rabbit vertebra! As a result of the obstruction, the upper lobe has collapsed, pneumonia has developed and the pleural surface is covered by fibrinous exudate.

Item no. MP2053

Fibrocaseous Tuberculosis

The left lung is cut longitudinally to display the cut surface. The upper lobe is almost entirely replaced by several large irregular cavities lined by necrotic debris and fibrous tissue. Blood vessels are seen in the upper cavity with evidence of haemorrhage. The lower lobe contains several smaller caseous areas, some of which are breaking down. The intervening lung parenchyma is scarred. The pleura is thickened. This is fibrocaseous tuberculosis with cavitation.

Item no. MP2054

Metastatic Tumour in Lung from Primary Testicular Cancer

This right lung specimen (and portions of 4 ribs) has been sliced longitudinally. There are numerous rounded tumour nodules evident in the lung parenchyma ranging from 5 to 30mm in diameter. The tumours are variegated in appearance with pale yellow and dark brown cut surfaces.

Item no. MP2055

Metastatic carcinomaa

The left lung has been sliced longitudinally to display the cut surface. Multiple pale tumour nodules of varying size are scattered throughout the lung substance. Near the hilum several nodules are confluent. The hilar lymph nodes contain pale tumour tissue. Small tumour nodules can be seen beneath the thickened pleura.

Item no. MP2056

Lobar pneumonia

The specimen is a parasagittal section of the right lung and the boundaries between the three lobes are visible. The entire upper and middle lobes are congested and hyperaemic* causing the darker appearance. There are smaller foci in the left lung.

Item no. MP2057

Bronchopneumonia

The specimen is a parasagittal section of the left lung. There are patchy regions of focal consolidations and discolorations caused by congested and hyperaemic lung tissue distributed within both lobes; however, the upper lobe is more severely affected. The consolidation appears to be concentrated around the bronchioles, which are ectatic. The costal (pleural) surface of the upper lobe is especially discoloured.

Item no. MP2058

Tracheoesophageal Fistula and Oesophagus Atresia

The specimen comprises the tongue, larynx, trachea, bronchi, both lungs and oesophagus of the foetus. The trachea and bronchi have been divided in the midline. A fistula is present just above the bifurcation at a communicating fistula can be seen connecting the distal oesophagus to the trachea (arrow). This is an example of a Type C Tracheoesophageal Fistula (oesophageal atresia with distal tracheoesophageal fistula).

Item no. MP2059

Right lung miliary tuberculosis

The right lung has been sliced longitudinally and mounted to display the cut surface. The bronchi and bronchioles are mildly ectatic. Scattered throughout the entire lung parenchyma are large numbers of small, pale yellows nodules less than 1 mm in diameter. Similar tiny subpleural nodules are seen on the surface of the visceral pleura. The nodules are tubercles. This is miliary tuberculosis, so-called due to the resemblance of the nodules to millet seeds.

Item no. MP2060

Lobar pneumonia - Grey Hepatisation Phase

The specimen is a parasagittal section of the right lung and the boundaries between the upper and lower lobes is clearly visible. The entire upper lobe is congested and pale grey in colour.

Item no. MP2061

Trachea — Hodgkin Lymphoma

The 3D print shows the tracheal bifurcation with adjacent paratracheal and peri-bronchial lymph nodes. The trachea has been opened longitudinally and is viewed from behind. The paratracheal lymph nodes are pale and matted (fused) together. Similar abnormal tissue is seen as a confluent pale mass on the left side of the trachea, above the aortic arch, which is seen cut in cross-section as a void space with branches arising.

Item no. MP2062

Lung — Cystic Fibrosis

The lung parenchyma shows extensive changes mainly with a bronchial distribution. Many bronchi are dilated (bronchiectasis) and contain thick, yellowish, purulent material. These changes are most marked in the upper lobe, at the apex of which a small focus of 'honeycomb' change is also seen. Multiple abscesses are present, especially in the basal and central parts of the lower lobe. The base of the lower lobe is severely affected with fibrosis and consolidation being evident.

Item no. MP2063

Lung - Staphylococcus aureus Abscesses

The right lung has been bisected. There are multiple irregular abscess cavities visible. The largest of these, in the apex of the lower lobe, measures 4 x 3 cm in diameter. At the apex of the upper lobe, there is another irregular abscess cavity which is less obvious, approximately 3 x 2 cm in diameter surrounded by a zone of consolidation. A number of small abscesses are also seen.

Item no. MP2064

Lung - Multiple Secondary Carcinoma Deposits in The Lung and Pleura

The left intact lung has multiple pale tumour nodules of varying size are scattered throughout the lung substance. Near the hilum several nodules are confluent. The hilar lymph nodes contain pale tumour tissue. Small tumour nodules from 2mm to 2cm can be seen beneath the thickened pleura on the costal, mediastinal and diaphragmatic surfaces.

Item no. MP2065

Multiple Polyposis Coli

The specimens from this case consists of two segments of sigmoid colon. The mucosa of the bowel is studded with numerous sessile and pedunculated partially pigmented polyps up to 1.5 cm in maximum diameter. There is no macroscopic evidence of malignant change.

Item no. MP2070

Villous adenoma of colon

A 15 cm long segment of colon has been opened longitudinally to display a large sessile tumour with a velvety surface. The tumour measures 11 x 7 cm. in diameter and approaches to within 2 cm of the distal resection margin. The mucosa is otherwise normal. The serosal surface is unremarkable. Histological examination confirmed the presence of a villous adenoma.

Item no. MP2071

Ulcerative Colitis

The resected colon has been sliced open longitudinally to show the mucosal surface. There is extensive confluent ulceration separated by oedematous islands of residual mucosa. The ulcers have necrotic bases with overhanging edges some of which form 'pseudo'-polyps. Histology of the bowel mucosa showed acute inflammatory changes with crypt abscesses, focal necrosis and ulceration. This is an example of acute ulcerative colitis (UC).

Item no. MP2074

Fatty Liver

A slice of liver reveals the characteristic yellow/grey and greasy appearance on one side. On the other side the appearance is restricted to the outer margin whilst the central area displays darker colouration possibly due to cirrhosis. This is an example of fatty change in the liver.

Item no. MP2072

Liver cirrhosis

A slice of liver has been mounted to display the cut surface, which shows multiple well demarcated nodules varying in size from 1 to 7 mm in diameter. The external surface of the liver is also nodular and irregular. This is an example of cirrhosis of the liver, with a mixed micro- and macronodular pattern and marked fatty change.

Item no. MP2073

Cholelithiasis (Gallstones)

The specimen is a portion of liver with attached gallbladder, which has been opened to display six large faceted mixed calculi. This is an example of cholelithiasis (gallstones).

Item no. MP2075

Chronic Gastric Ulcer

The specimen is a 2cm coronal slice of tissue, which incorporates a portion of stomach diaphragm, liver and pancreas. The specimen has been opened to display a large ulcer at the upper end of the lesser curvature near the gastro-oesophageal junction. Macroscopically, the loss of substance at the site of the ulcer is oval, has 5-6cm in diameter and slightly elevated borders. The base is clean and smooth with no evidence of haemorrhage.

Item no. MP2076

Intussusception of small bowel due to metastatic tumour

The specimen is a segment of small bowel, approximately 20 cm in length, with attached mesentery up to 2 cm in width (more evident on the uncut aspect of the specimen). About 5 cm from the proximal surgical resection margin (which is at the left hand of the specimen), a polypoid tumour 3 cm in diameter has become invaginated into the lumen of the bowel, and has been propelled distally, forming an intussusception 13 cm in length. The tumour is seen at the apex of the intussusception (near the right hand side of the specimen). The congestion and exudate seen on the mucosal surface of the intussusception (invaginated portion) are features considered with early ischaemic necrosis. The histological diagnosis is not recorded in this case; however, the macroscopic appearance is consistent with a metastatic malignant tumour, although the possibility of a primary tumour cannot definitely be excluded.

Item no. MP2077

Gall Stone Ileus

This segment of small bowel has been opened to display a large pigmented, ovoid gall stone with a roughened surface. This is an example of gall stone ileus.

Item no. MP2078

Hirschsprung's Disease

This postmortem section of sigmoid colon has been opened to display the internal surface shown here. There is large dilation of the proximal section of bowel (sigmoid) with loss of the normal mucosal pattern. The distal section of bowel (rectum) has a normal diameter and a normal mucosal pattern but an absence of ganglion cells in the myenteric plexus. This is an example of Hirschsprung's disease, also known as congenital aganglionic megacolon.

Item no. MP2079

Pedunculated Adenoma of the Colon

This specimen is the resected segment of descending colon. There is a single dark lobulated mass visible arising from the mucosal surface. It is attached to a stalk which is 4cm in length. Histologically, the mass comprises a core of connective tissue covered with hyperplastic glandular epithelium of colonic type, with focal nuclear atypia. This is an example of a tubular colonic adenoma.

Item no. MP2081

Adenocarcinoma of the stomach

This is a post mortem specimen sliced to include a sagittal view of the oesophagus, stomach, proximal duodenum and pancreas. A large 7x5cm ulcer is evident on the lesser curve of the stomach. The ulcer is shallow and broad with raised rolled edges and necrotic debris at the base. There is loss of gastric rugae radiating along the mucous from the ulcer. Dissection of the ulcer reveals elevation of the edge by pale homogenous tumour tissue. There were two eroded arteries present within the ulcer crater with evidence of recent haemorrhage. The pancreas is adherent to the serosal aspect of the ulcer. Histology taken from the lesion (sites visible as regular 3cm defects) demonstrated an ulcerating, well-differentiated adenocarcinoma of the stomach with direct invasion into the pancreas.

Item no. MP2080

Cholecystitis and Cholelithiasis

A thick-walled gallbladder has been opened to display a thickened haemorrhagic mucosa and many irregular faceted calculi. A large calculus is impacted in the neck of the gallbladder. The serosal surface of the gall bladder is congested and has lost its normal sheen. This is an example of cholecystitis complicating cholelithiasis (gallstones).

Item no. MP2082

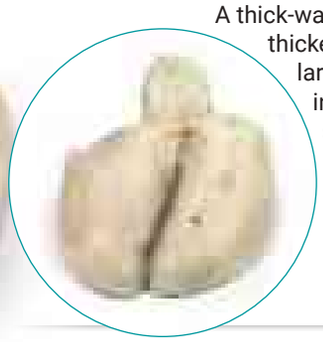

Mesenteric Metastases from Cutaneous Malignant Melanoma

The specimen is a loop of small intestine mounted to display the mesentery, which contains numerous small dark brown, circumscribed nodules varying from pin head size to approximately 1 cm in diameter. Histology confirmed the diagnosis of metastatic melanoma.

Item no. MP2083

Hepatic duct calculi and Obstructive Biliary Cirrhosis

The specimen is a slice of liver mounted to display the cut surface. The capsule is slightly thickened and the liver substance has a finely nodular appearance. Intrahepatic bile ducts are dilated. When the posterior or inferior surface is viewed an irregular pigmented calculus, 10 mm in diameter, is seen impacted in a distended hepatic duct. Another smaller calculus 3 mm in diameter has been dislodged. This specimen represents an example of secondary biliary cirrhosis due to large duct obstruction from hepatic calculi.

Item no. MP2084

Hepatocellular Carcinoma

This is the liver specimen of the patient on postmortem examination. The cut surface of the liver has a multinodular appearance consistent with macronodular cirrhosis. These multiple nodules are of varying size up to 2cm in diameter, and are separated by narrow bands of fibrous tissue. There are two large round tumours also visible. These are 8cm and 6cm in diameter with a variegated cut surface due to focal necrosis, haemorrhage and bile staining. This is an example of hepatocellular carcinoma that has developed on the background of a cirrhotic liver.

Item no. MP2085

Adrenal haemorrhage / Waterhouse-Friderichsen Syndrome

The combined kidney and adrenal gland have been mounted, in order to display the cut surfaces. Extensive haemorrhage has occurred into the adrenal medulla, and there is some extravasation of blood into the periadrenal fat. This is an example of adrenal haemorrhage in the setting of severe septic shock also known as 'Waterhouse-Friderichsen' syndrome.

Item no. MP2090

Adult polycystic kidney disease

The specimen is an enlarged kidney. The renal parenchyma has been almost completely replaced by numerous dilated cysts varying in size, up to 3cm in diameter. The cysts have thin translucent walls, and some cysts contain material of varying colours, giving a 'marble-like' appearance to the cut surface of the kidney.

Item no. MP2091

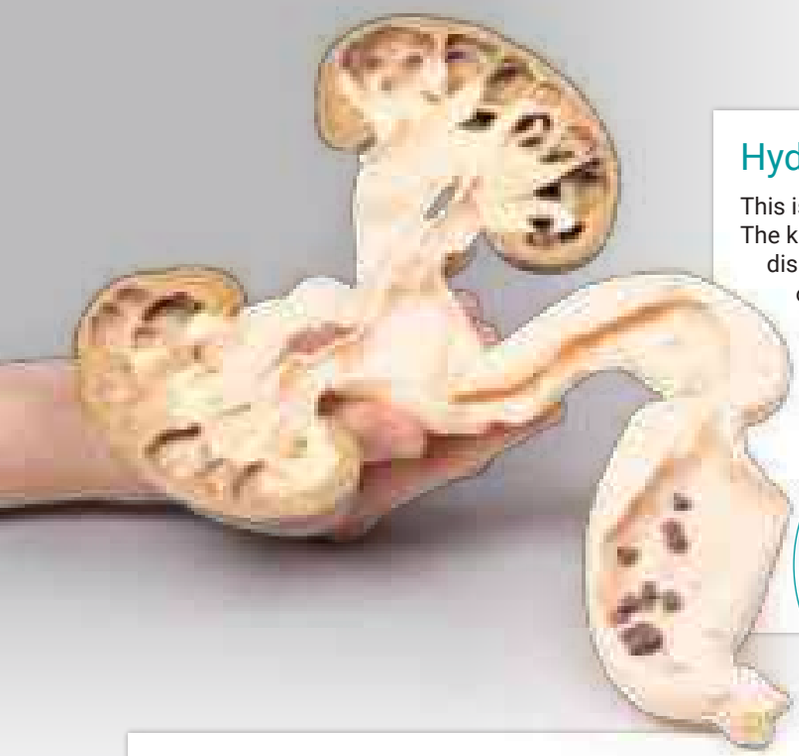

Hydronephrosis Hydroureter

This is the patient's left nephrectomy and ureterectomy specimen. The kidney has been bisected and the cut surface of both halves is displayed, mounted in continuity with the ureter, which has been opened. The kidney is grossly hydronephrotic, and there is considerable atrophic thinning and loss of renal parenchymal tissue. The ureter is extremely dilated and distally contains a number of small brown-black calculi with irregular sharp surface projections. These are calcium oxalate stones.

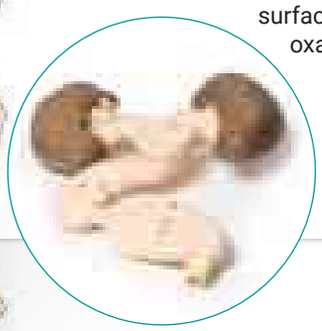

Item no. MP2093

Horseshoe Kidney

The kidney is 12 cm in length and the two parts are fused at the lower pole forming this horseshoe-like shape. The ureters can be seen emerging from the hilum on the anterior aspect of the 3D print. The kidney is bisected in the horizontal plane which is evident on the posterior aspect.

Item no. MP2092

Hydronephrosis and Hydroureter Caused by Obstruction by a Renal Calculus

The specimen is patient's right kidney, which is grossly and partially bisected. There is gross dilatation of the pelvi-calyceal system visible and significant atrophy of renal tissue particularly in the cortex. There is a large brown calculus visible in the renal pelvis at the ureteropelvic junction.

Item no. MP2094

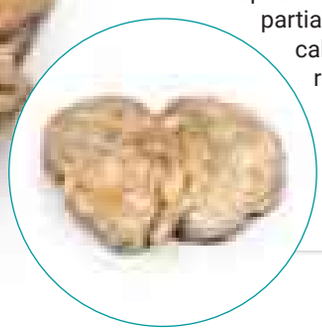

Multiple Renal Calculi

The specimen is patient's kidney, which is grossly and partially bisected. There is gross dilatation of the pelvi-calyceal system visible. Significant atrophy of renal tissue can be seen, in some places being reduced to a mere rim. A large mottled brown-white calculus lies in the pelvis, and a smaller calculus occludes the ureter lumen. The ureter is dilated proximal to the impacted calculus. There are multiple calculi visible within the calyces of the specimen.

Item no. MP2095

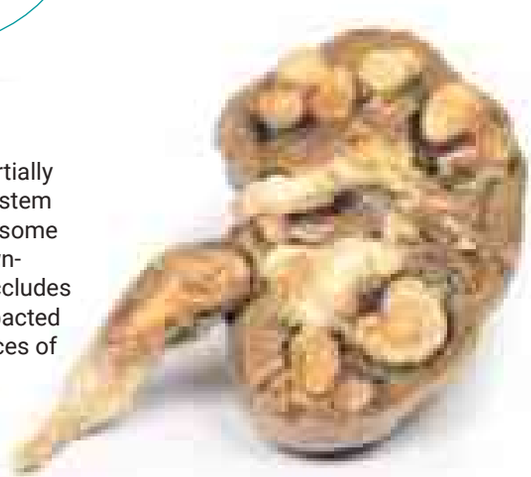

Pyonephrosis

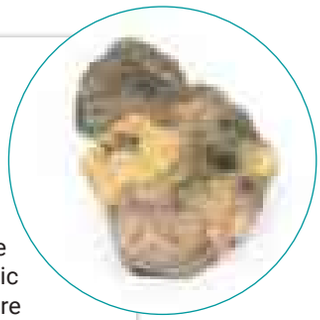

This is the patient's left nephrectomy specimen. The kidney has been sliced to display the cut surface. The pelvis and calyces are greatly dilated, and contain remnants of yellow pus. There is considerable fibrosis of the renal parenchyma. In the mid-zone near the lateral border, there is a hemorrhagic necrotic area 35 x 12 mm in diameter containing pus. There are two similar small hemorrhagic necrotic areas visible on the capsular surface.

Item no. MP2096

Renal Cell Carcinoma

The specimen is a kidney, which has been incompletely dissected in the coronal plane, and mounted to display the cut surface. The lower pole of the kidney has been replaced by a rounded ill-defined irregular mass 5cm in diameter, which has compressed and distorted the overlying renal parenchyma. The cut surface of the tumour has a variegated appearance caused by areas of haemorrhage and necrosis. Several small pale-yellow tumour nodules are present in the cortex and medulla above and separate from the lower pole tumour.

Item no. MP2097

Septic Renal Infarct

The specimen is the patient's kidney from post mortem examination. The kidney has been bisected with a cut half surface on display. There are multiple well demarcated wedge shaped pale yellow-white areas evident within the cortex. The base of these pyramids lies against the cortical surface and extend along the renal columns with the apex pointing toward the medulla. The largest is evident lateral upper pole of the kidney. Theses pale areas are infarcted renal tissue. There are dark irregular shaped areas which represent areas of hemorrhage.

Item no. MP2098

Papillary Transitional Cell Carcinoma of the Renal Pelvis

This is the post-nephrectomy kidney. Of note the kidney maintains its foetal lobulation. There is a friable papillary tumour of 35mm in diameter projecting in the renal pelvis. The renal pelvis is visibly dilated due to this obstructing tumor. Histological examination revealed this is papillary transitional cell carcinoma arising in the renal pelvis.

Item no. MP2099

Lymphoma of the thyroid

The larynx, thyroid, upper trachea and oesophagus are included in the specimen. The enlarged left lobe and to a lesser degree, the right lobe of the thyroid, are replaced by homogeneous pale tumour tissue. Stretched over the lateral margin of the left lobe is the common carotid artery. Note on the internal aspect how the larynx is compressed and the oesophagus virtually disappears into the bulk of the tumour. The histological appearance of the tumour was consistent with lymphoblastic lymphoma of the thyroid.

Item no. MP2100

Multinodular goitre

The specimen, removed at post-mortem, includes the base of the tongue, larynx and trachea. It has been cut in the coronal plane to allow a view of the internal laryngeal and tracheal anatomy. The thyroid gland is grossly enlarged particularly the right lobe, which extends superiorly and inferiorly, well beyond its normal margins when viewed from the anterior aspect. The cut posterior surfaces display many hyper- and hypopigmented nodules as well as cystic areas in both lobes. The tongue base, larynx and trachea appear relatively normal.

Item no. MP2101

Aorta & para-aortic lymph nodes

The specimen consists of the abdominal aorta and common iliac arteries surrounded by large numbers of extremely enlarged iliac nodes para-aortic lymph nodes. Histopathological examination revealed metastatic high-grade adenocarcinoma in some of the resected lymph nodes.

Item no. MP2103

Retrosternal Goiter

The specimen, removed at post-mortem, includes the larynx, trachea and large multilobular thyroid gland. The thyroid gland is grossly enlarged particularly the right lobe, which has two large lobes extending superiorly and inferiorly for a range of 7-8mm, well beyond its normal margins when viewed on anterior aspect. Posteriorly, the oesophagus has been opened to expose the posterior wall of the trachea. The right lobe presents as larger than from the anterior perspective, and the abnormal growth appears to be mainly the inferior pole of the right lobe. The surfaces do not display major pigmentary changes. Prominent veins are visible on the surface of the right lobe.

Item no. MP2102

Nodular hyperplasia of the Prostate

The specimen is an enlarged prostate gland sliced transversely to display the external and cut surfaces, On the cut surface there are numerous nodules varying in size from 2-10mm in diameter. This is an example of benign nodular hyperplasia (BPH) of the prostate gland.

Item no. MP2108

Uterus Bicornuate Unicollis

This hysterectomy specimen is of a bicornuate uterus, fallopian tubes and ovaries; sliced coronally and mounted to display cut and external surfaces. Both uterine bodies are equal in size and share a common cervical canal. A few small cysts are present in the cervix.

Item no. MP2104

Carcinoma of Breast

The specimen is the patient's left breast mounted to display the cut surface. Immediately beneath and attached to the skin is a large oval tumour mass 11cm in maximum diameter. The tumour is adherent to the underlying muscle. The tumour is not encapsulated and has a variegated cut surface with areas of necrosis, haemorrhage and cyst formation. This is a breast adenocarcinoma, which involved the regional lymph nodes.

Item no. MP2105

Endometrial Carcinoma

The specimen consists of uterus, fallopian tubes and ovaries. The endometrial cavity and endocervical canal have been opened on the anterior aspect. The endometrial lining is grossly abnormal especially on the right side and a brown polypoid tumour has invaded the myometrium and extends inferiorly into the cervical canal. Histologically this was a well-differentiated adenocarcinoma of the endometrium.

Item no. MP2106

Uterine Leiomyoma

The specimen includes the cervix, body and fundus of the uterus. The uterus, which is of normal size, has been cut in the sagittal plane. A large ovoid mass approximately 4cm x 2cm protrudes into the uterine cavity and extends as far inferiorly as the opening of the cervix. It originates from the posterior aspect of the uterus. The cervical canal is clearly visible.

Item no. MP2107

Hydrocoele

The specimen is a testis and its coverings, sliced to display the cut surface. The cavity bounded by the visceral and parietal layers of the tunica vaginalis is distended due to the accumulation of serous fluid. This is an example of a hydrocoele, secondary to generalised oedema due to congestive cardiac failure.

Item no. MP2109

Chronic hydrocoele

The specimen consists of a testis, tunica vaginalis and distal end of the spermatic cord. The testis and its surrounding layers have been bisected to display the cut surface. The tunica vaginalis is thickened and the enclosed cavity is distended. The testis is normal. This is an example of a chronic secondary communicated hydrocoele.

Item no. MP2110

Tuberculosis

The specimen is a portion of the patient's thoracic vertebral column that has been sawn longitudinally and mounted to display the cut surface of 7 thoracic vertebrae. In all vertebrae, there are osteolytic areas, varying from 1 to 12 mm in diameter, which contain caseous degenerative material* (mostly now lost) and are surrounded by a thin zone of dense bone. The tuberculous inflammatory process has extended into one of the intervertebral discs, and has also spread outside the vertebral bodies to form collections of caseous material beneath the anterior longitudinal ligament.

Item no. MP2111

Chondrosarcoma of femur and ilium

The specimen consists of the upper end of the femur and its articulation with the pelvis. Within the neck and head of the femur and replacing most of the ilium there is a lobulated pale grey tumour with areas of cavitation, necrosis and haemorrhage. The tumour is extending out beyond bone into the surrounding soft tissues and appears encapsulated. The presence of infiltration, necrosis and haemorrhage are macroscopic features of malignancy.

Item no. MP2112

Tertiary Syphilis

This specimen is the vault of the patient's skull. On the external surface, there are multiple circumscribed necrotic lesions in the parasagittal area to the left of the midline. The lesions are brown in colour and measure up to 3-4 cm in maximum diameter. The lesions have eroded the outer table of the skull and the adjacent periosteum is thickened with a fibrinous inflammation.

Item no. MP2113

Chondrosarcoma of scapula

The specimen is the patient's excised right scapula. An irregular lobulated tumour 11 cm in maximum diameter arises from the spine of the scapula and extends to involve the acromion and coracoid process. The tumour is a mottled pale-yellow brown colour with patchy surface haemorrhage. There is some adherent muscle and fibrous tissue. The mass has infiltrated and replaced the normal bone. Histologically the tumour consisted of pleomorphic rounded and spindle-shaped cells with numerous mitotic figures and cartilage formation. This is chondrosarcoma of the scapula.

Item no. MP2114

Osteosarcoma of femur

The specimen is the patient's excised distal femur. On the cut surface, there is a large pale infiltrating tumour, 10 cm in greatest diameter, extending through the periosteum near the articular surface. This is an osteosarcoma of the femur.

Item no. MP2115

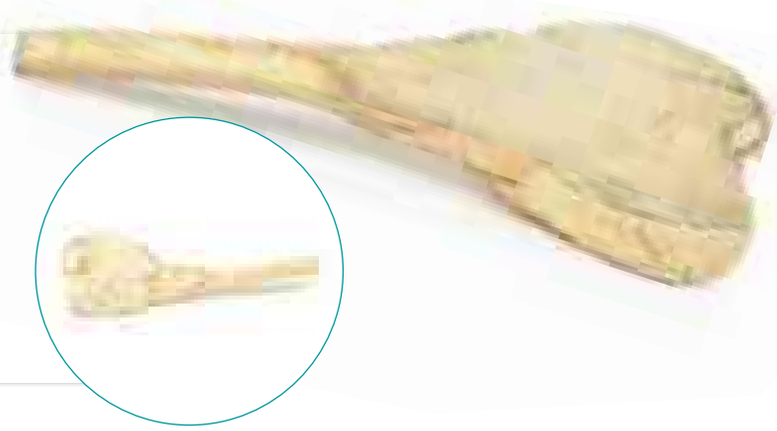

Chondrosarcoma

The specimen comprises the head, neck and upper third of the shaft of the right femur, sawn longitudinally to display the cut surface. In the medullary cavity of the upper portion of the shaft is an ovoid tumour that is 6.5 cm in maximum diameter. The tumour is not encapsulated and has a haemorrhagic cut surface with pale hyaline and cystic areas. Histologically, this is a low grade chondrosarcoma.

Item no. MP2116

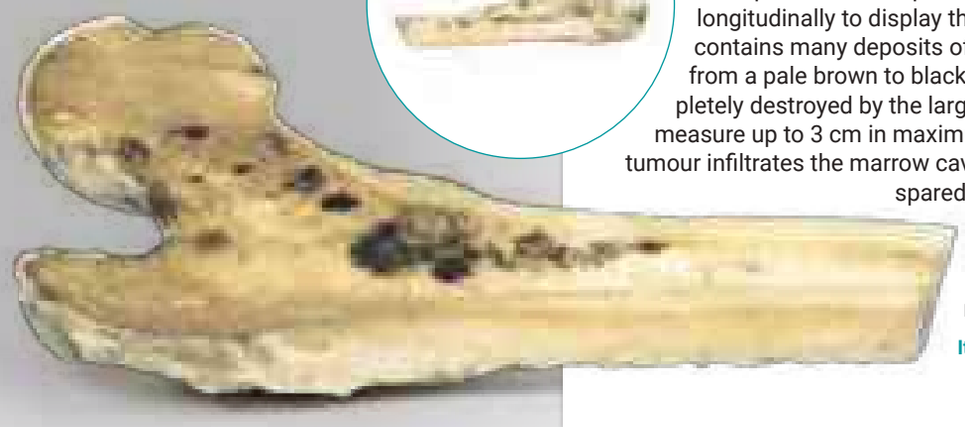

Metastatic Malignant Melanoma

The specimen is the patient's proximal right femur sawn longitudinally to display the cut surface. The medullary cavity contains many deposits of tumour tissue varying in colour from a pale brown to black. Cancellous bone has been completely destroyed by the larger deposits, which appear dark and measure up to 3 cm in maximum diameter. Elsewhere pale brown tumour infiltrates the marrow cavity diffusely. Cortical bone has been spared, although at the junction of the shaft and neck, medially the cortical bone is discoloured and thickened. These are metastatic deposits from a melanoma of the skin.

Item no. MP2117

Osteochondroma

The specimen is the lower end of the patient's right femur, which has been cut in the coronal plane and mounted to display the external surfaces. A pedunculated bony protuberance 2 cm in length projects from the medial aspect of the femoral shaft 7 cm above the medial condyle. The projection is composed of normal bone with a thin cap of hyaline cartilage at the tip. This is an example of an osteochondroma.

Item no. MP2118

Suppurative arthritis of the knee

The specimen displays the articular surfaces of a femur and tibia. The articular surfaces have been severely eroded. They are brown in colour, very irregular, and there are shaggy adhesions and plaques of yellow necrotic material. No normal articular cartilage is present. Some irregular varying in size bony projections (up to 1 cm in diameter) are present on the femoral condyles. Staphylococcus aureus was cultured from the joint. This is an example of suppurative arthritis in a joint previously damaged by tuberculosis.

Item no. MP2119

Erler-Zimmer GmbH & Co.KG
Hauptstraße 27 · D-77886 Lauf
Phone: (+49) 07841/67191-0 · Fax: (+49) 07841-67191-99
E-Mail: info@erler-zimmer.de · www.erler-zimmer.de
www.3danatomyseries.com

Experts in medical education since 1950

ERLER ZIMMER

Follow us!